Ribosomal protein L14 contributes to the early assembly of 60S ribosomal subunits in *Saccharomyces cerevisiae*

Francisco Espinar-Marchena[1,†], Olga Rodríguez-Galán[1,†], José Fernández-Fernández[1], Jan Linnemann[2] and Jesús de la Cruz[1,*]

[1]Instituto de Biomedicina de Sevilla (IBiS), Hospital Universitario Virgen del Rocío/CSIC/Universidad de Sevilla, and Departamento de Genética, Universidad de Sevilla, Seville, Spain. Avda. Manuel Siurot, E-41013 Seville, Spain and [2]Institut für Biochemie III, Universität Regensburg, 93053, Regensburg, Germany

ABSTRACT

The contribution of most ribosomal proteins to ribosome synthesis has been quite well analysed in *Saccharomyces cerevisiae*. However, few yeast ribosomal proteins still await characterization. Herein, we show that L14, an essential 60S ribosomal protein, assembles in the nucleolus at an early stage into pre-60S particles. Depletion of L14 results in a deficit in 60S subunits and defective processing of 27SA$_2$ and 27SA$_3$ to 27SB pre-rRNAs. As a result, 27S pre-rRNAs are subjected to turnover and export of pre-60S particles is blocked. These phenotypes likely appear as the direct consequence of the reduced pre-60S particle association not only of L14 upon its depletion but also of a set of neighboring ribosomal proteins located at the solvent interface of 60S subunits and the adjacent region surrounding the polypeptide exit tunnel. These pre-60S intermediates also lack some essential *trans*-acting factors required for 27SB pre-rRNA processing but accumulate practically all factors required for processing of 27SA$_3$ pre-rRNA. We have also analysed the functional interaction between the eukaryote-specific carboxy-terminal extensions of the neighboring L14 and L16 proteins. Our results indicate that removal of the most distal parts of these extensions cause slight translation alterations in mature 60S subunits.

INTRODUCTION

Ribosomes are ubiquitous ribonucleoprotein particles that are responsible of protein synthesis. In all organisms, ribosomes are composed of two ribosomal subunits (r-subunits), the large one being about twice the size of the small one ([1](1)). The structures of ribosomes from prokaryotes and eukaryotes have been resolved at atomic resolution ([2](2)). Globally, eukaryotic ribosomes are much larger and complex than prokaryotic ones due to the presence of additional rRNA sequences, named expansion segments (ESs), and the addition of several eukaryote-specific r-proteins ([2](2)) and r-protein extensions (see ([3](3)) and references therein). Ribosomes are not homogeneous entities; indeed both in prokaryotes and eukaryotes, multiple examples of ribosome heterogeneity, including variations in the r-protein complement, alternative rRNA molecules, differential degree of r-protein and/or rRNA modification, and presence of more than one copy of selected r-proteins per subunit, have been reported (e.g. ([4–7](4))).

Ribosome synthesis is a highly energy-consuming and dynamic process ([8,9](8)). In eukaryotes, the synthesis of cytoplasmic ribosomes is a compartmentalized pathway that takes place largely in the nucleolus (for reviews, see ([10,11](10))), although late steps occur in the nucleoplasm and in the cytoplasm ([9,12,13](9)). Ribosome synthesis proceeds *via* the formation of pre-ribosomal intermediates ([14](14)) that contain r-proteins and many non-ribosomal RNA or protein factors, known as ribosome assembly or *trans*-acting factors, which provide speed, accuracy, and directionality to this pathway ([15,16](15)). Within these pre-ribosomal particles and along the maturation path, the precursors rRNAs (pre-rRNAs) are modified, processed, and folded (see Supplementary Figure S1); concomitantly, the r-proteins assemble in a hierarchical manner. Thus, distinct r-proteins, the so-called primary binding proteins, stably bind directly to the nascent pre-rRNAs, while secondary and ternary binding proteins require the previous binding of one or more r-proteins ([8,9](8)). Apparently, the initial interactions of r-proteins with nascent pre-rRNAs are weak but become reinforced as assembly proceeds (e.g. ([17–19](17))). Different reports have given rise to the interpretation that assembly of r-proteins oc-

*To whom correspondence should be addressed. Tel: +34 95 592 31 26; Fax: +34 95 592 31 01; Email: jdlcd@us.es
†These authors contributed equally to this work as first authors.

curs *via* the hierarchical but nonlinear formation of discrete folding modules or blocks containing neighboring r-proteins and rRNAs, which respectively assemble or fold in an interdependent fashion (e.g. (17,20,21)). In *S. cerevisiae*, the eukaryote where ribosome biogenesis has perhaps been best studied (10), the course of r-protein assembly has been tackled *in vivo* by different approaches. (i) The pioneering work investigated the order in which r-proteins are incorporated into early or late nuclear pre-ribosomal particles. From these studies, it became evident that r-proteins can be grouped roughly into three classes: most r-proteins assemble early into distinct 66S and 43S nucleolar pre-ribosomal particles, some r-proteins are added later but still in the nucleus, and few r-proteins assemble in the cytoplasm (22,23). (ii) The timing of r-protein assembly has tentatively been deduced by the compositional analyses of distinct pre-ribosomal particles purified using selected tagged *trans*-acting factors as baits by affinity purification methods, especially by the TAP procedure (e.g., see (24–27)). The fact that r-proteins were found as frequent contaminants of TAP purifications of protein complexes (e.g. (28,29)) made these results less reliable until the use of more careful analyses of affinity purification and/or protein identification methods (e.g. (17,19,30)). (iii) The timing of r-protein assembly has also been studied by the affinity purification of complexes using specific tagged r-proteins as baits and the determination of the co-purified pre-rRNA intermediates (e.g. (31–33)). (iv) The *in vivo* function of most r-proteins in ribosome assembly has also been studied by the examination of the defects in pre-rRNA processing and nucleocytoplasmic export of pre-ribosomal particles upon their depletion (for few representative examples, see (34–39)). From these studies, r-proteins were classified as early-, intermediate-, late- or cytoplasmically-acting components affecting specific steps of ribosome maturation. In some cases, in addition to pre-rRNA processing and export of pre-ribosomal particles, the changes in the protein composition, *trans*-acting factors and r-proteins, of pre-ribosomal particles upon depletion of selected r-proteins have also been determined (17,19,21,40). Together, these studies indicate that the timing of action of r-proteins remarkably correlates with their specific location within mature r-subunits and provide a scenario of the sequential assembly of r-proteins (see below). (v) The interaction of each r-protein with the rRNAs and other r-proteins within yeast mature ribosomes has been resolved at atomic resolution (41–43). Importantly, the structure of many ribosome assembly intermediates has also been elucidated by cryo-electron microscopy (cryo-EM) at near-atomic resolution (e.g. (44–51), reviewed in (52–54)). The comparison of the structures of these intermediates with that of the respective mature r-subunits and/or the structure that some r-proteins adopt when bound to their specific chaperones (e.g. (55–57)) is providing for the first time molecular clues about how r-proteins undergo different structural rearrangements to acquire their final and stable position within mature r-subunits. These rearrangements are best exemplified by the incorporation of the 5S RNP into early pre-60S r-particles and its rotation to reach its final position in mature 60S r-subunits (45,58,59). Altogether, all these approaches have ended with the following model for the maturation of the r-subunits (reviewed in (9)). The small r-subunit seems to assemble in a bipartite manner: first, the co-transcriptional formation of the body of the r-subunit occurs, comprising the association of the set of r-proteins that bind the 5′ domain of 18S rRNA; later, the formation of the head of the r-subunit takes place by the assembly of those r-proteins that bind the 3′ domain of the 18S rRNA. The construction of the head structure is necessary for the proper export of the pre-40S r-particle to the cytoplasm, where the assembly of the last r-proteins occurs (17,39). This outline has largely been preserved in higher eukaryotes (60) and it is reminiscent of the classical *in vitro* assembly pathway initially established by M. Nomura and co-workers (8,61). The development of new purification techniques for capturing assembly intermediates of 90S pre-ribosomal particles (62,63) and the cryo-EM determination of intermediates during the maturation of small r-subunits (49,64–66) will certainly help, besides other approaches, to improve our understanding of small r-subunit assembly. The large r-subunit assembles hierarchically and its construction occurs parallel to the maturation of the 25S/5.8S rRNAs (see Supplementary Figure S1). The earliest assembly steps of large r-subunit likely involve the initial compaction of $27SA_2$ pre-rRNA aided by the binding of at least primary r-protein L3 (uL3 according to the recently proposed r-protein nomenclature (67)). Next, and coupled to the removal of ITS1, those r-proteins that bind mainly domains I and II in the 25S/5.8S rRNAs associate with the particles. All these r-proteins, including L4, L6, L7, L8, L9, L13, L16, L18, L20, L32 and L33 (uL4, eL6, uL30, eL8, uL6, eL13, uL13, eL18, eL20, eL32 and eL33, respectively), form a belt around the equator of the solvent-exposed surface of the large r-subunit. Intermediate steps of assembly include cleavage at the C_2 site in the ITS2 spacer and association of some r-proteins in the vicinity to 5.8S rRNA and the perimeter of the solvent-exposed part of the peptide exit tunnel, among them L17, L19, L23, L26, L27, L35 and L37 (uL22, eL19, uL14, uL24, eL27, uL29 and eL37, respectively). It has been reported that association of L2, L39 and L43 (uL2, eL39 and eL43, respectively) with pre-60S r-particles is likely specifically stabilized after cleavage at the site C_2, an event that might require the previous assembly of the above middle-acting r-proteins. The next reactions in 60S r-subunit assembly are described as late nuclear steps and include the maturation of 25.5S and 7S pre-rRNAs and the rotation about 180° of the central protuberance, which contains 5S rRNA and r-proteins L5 and L11 (uL18 and uL5, respectively), to acquire its final conformation in mature r-subunits. At this stage, pre-60S r-particles are competent for nuclear export. The final steps of assembly occur in the cytoplasm and include, among other events, the processing of 6S pre-rRNAs to mature 5.8S rRNAs and the assembly of few r-proteins, among them L10, L24, L29, L40, L42, P1 and P2 (uL16, eL24, eL29, eL40, eL42, P1 and P2, respectively), which are located at the r-subunit interface (for references, see (9,19,21,68)). As for 40S r-subunits, the sequence of r-protein incorporation into 60S r-subunits has been well conserved in higher eukaryotes (69).

The role of few r-proteins in pre-rRNA processing and ribosome assembly remains undefined or has only been poorly characterized. Among these orphan proteins is L14 (eL14). L14 is an eukaryote-specific r-protein from the 60S r-subunit, which is conserved in some but not all archaea

(1,70). In addition, eukaryotic L14 contains a specific C-terminal extension absent in the archaeal orthologues (71), whose role is unknown. L14 forms a eukaryote-specific structure, close to the r-stalk, on the solvent-exposed surface of the 60S r-subunits together with the ES7^L and ES39^L of domain II and VI of 25S rRNA, respectively, H41 of domain II of 25S rRNA, its interacting r-proteins L6, L9, L16, L20, and its neighboring r-proteins L7, L32 and L33. (Supplementary Figure S2). Knockdown of *RPL14* expression by siRNA in human cells impairs 28S and 5.8S rRNA synthesis and formation of 60S r-subunits (69,72). In this study, we have examined the precise role of the otherwise uncharacterized yeast L14 r-protein in ribosome biogenesis. Our data indicate that yeast L14 assembles in the nucleolus within the earliest pre-60S r-intermediates. Depletion of L14 causes a shortage of 60S r-subunits, which is due to defective production and accelerated turnover of early and intermediate pre-60S r-particles. Consistently, pulse-chase analyses demonstrate impaired production of mature 25S and 5.8S rRNAs, northern blot hybridization shows mild accumulation of 27SA pre-rRNAs and low steady-state of 27SB and 7S pre-rRNAs, and fluorescence microscopy suggests a defect in the nuclear export of pre-60S r-particles. We have also analysed the impact of L14 depletion on the protein composition of early pre-60S r-particles, which were affinity-purified using TAP-tagged Noc2 as bait. Our results clearly show that L14 is required for the stable assembly of a subset of r-proteins, mainly located in its immediate neighborhood, such as L6, L20 and L33 or surrounding the solvent-exposed part of the peptide exit tunnel such as L17, L26, L37 and L39. L14 is also particularly required for the association of few late-acting ribosome assembly factors, most of them essential for cleavage at site C_2 in ITS2. Finally, we also discuss the role of the eukaryote-specific C-terminal extension of yeast L14 in ribosome biogenesis and function.

MATERIALS AND METHODS

Strains and microbiological methods

The *S. cerevisiae* strains used are listed in Supplementary Table S1 and are derived from W303. The deletion disruption of the *RPL14A* and *RPL14B* genes and the C-terminal TAP-tagging of *NOC2* at the genomic locus were performed as previously described (19,73). FEY204 (*rpl14A*::HIS3MX6) and FEY203 (*rpl14B*::HIS3MX6) are meiotic segregants of the corresponding diploid strains. To construct the *GAL::RPL14* strain, FEY203 and FEY204 were crossed and the resulting diploid transformed with the YCplac33-RPL14A plasmid. After sporulation and tetrad dissection, we selected the FEY229 strain, which is a representative double *rpl14Δ rpl14BΔ* mutant that contains YCplac33-RPL14A. Then, FEY229 was transformed with the pAS24-RPL14A plasmid, and, subsequently, YCplac33-RPL14A was counter-selected on 5-FOA plates containing galactose. The correct genomic integration of the *TAP-URA3* cassette in the wild-type and FEY320 strains was verified by PCR and the expression of the Noc2-TAP fusion protein by western blot analysis. Strains JFY136 and JFY137 are also meiotic segregants; YKL516 and JFY01 were crossed, the resulting diploid was

sporulated, and tetrads were dissected. In spore clones with the appropriate markers, the presence of the wild-type or mutant variant alleles of *RPL14A/B* and *RPL16A/B* genes were analysed by PCR. The expression of the wild-type L14A and L16B or the truncated variants L14A-N122 and L16B-N180 proteins was tested by western blot analysis. Information on the crosses between strains harboring the *mak5Δ, ebp2Δ* or *nop16Δ* deletions and strains harboring the *rpl16B-N180*, *rpl14A-N122* or the *rpl6AΔ* alleles is provided in the legends to Supplementary Figures S12–S14.

Strains were grown at selected temperatures either in rich YP medium (1% yeast extract, 2% peptone) supplemented with 0.2% adenine and containing either 2% glucose (YPD) or 2% galactose (YPGal) as carbon source or in synthetic minimal medium (0.15% yeast nitrogen base, 0.5% ammonium sulphate) supplemented with the appropriate amino acids and bases as nutritional requirements, and containing either 2% glucose (SD) or 2% galactose (SGal) as carbon source. Preparation of media and genetic manipulations were done according to established procedures. Antibiotic-containing plates were prepared by adding the drugs from stock solutions into 2% YPD-agar medium before pouring the plates (74). Yeast cells were transformed by the lithium acetate method (75). Tetrad dissections were performed using a Singer MS micromanipulator.

Plasmids

All recombinant DNA techniques were done according to established procedures using *E. coli* DH5α for cloning and propagation of plasmids. Plasmids used in this study are listed in Supplementary Table S2. To construct YCplac33-RPL14A, YCplac111-RPL14A, YCplac111-rpl14A-N109, YCplac111-rpl14A-N97, pAS24-RPL14A, and YCplac111-RPL14A-yGFP, specific DNA fragments were PCR-amplified using yeast genomic DNA as a template and the appropriate oligonucleotides. The oligonucleotides used in this study are listed in Supplementary Table S3. After restriction digestion, the PCR products were cloned into the respective vectors. All cloned DNA fragments generated by PCR were verified by sequencing. Detailed information on the plasmids is available upon request. YCplac22-RPL14A, YCplac22-rpl14A-N122, YCplac22-MAK5, YCplac22-mak5-N723, YCplac22-mak5-N727, YCpla22-mak5-G218D, YCplac22-EBP2, and YCplac22-ebp2-N286, generous gifts from D. Kressler, have been previously reported (71). Other plasmids used in this study were: pRS314-RPL25-eGFP-NOP1-mRFP and pRS314-RPS3-eGFP-NOP1-mRFP, gifts from J. Bassler and E. Hurt, and pRS316-GAL-NMD3Δ100, gift from A. Jacobson (Supplementary Table S2).

Polysome profile analyses

Cell extracts for polysome profile analyses were performed as described previously (76). 7–50% sucrose gradients were centrifuged at 39 000 rpm in a Beckman Coulter rotor SW41 Ti at 4°C for 2 h 45 min and fractionated using a Teledyne-ISCO UA-6 system with continuous monitoring at A_{254}.

Pulse-chase labeling of pre-rRNA

Pulse-chase labelling of pre-rRNA was performed exactly as previously described (77), using 100 μCi of [5,6-³H]uracil (Perkin Elmer; 45–50 Ci/mmol) per 40 OD$_{600}$ of yeast cells. Cells were grown in SGal-Ura medium at 30°C to mid-log phase or shifted to SD-Ura medium for 6 h, pulse-labeled for 2 min and chased for different times with SD medium containing an excess of cold uracil. Total RNA was extracted by the hot acidic phenol–chloroform procedure (78). Radioactive incorporation was measured by scintillation counting and ∼20 000 cpm per RNA sample were loaded and resolved on 1.2% agarose–6% formaldehyde and 7% polyacrylamide–8 M urea gels. RNA was then transferred to nylon membranes and visualized by fluorography (77).

Steady-state analysis of pre-rRNA

Northern hybridization and primer extension analyses were carried out as previously described (77,79). Total RNA was extracted from samples corresponding to 10 OD$_{600}$ units of cells grown to mid-log phase. Equal amounts of total RNA were loaded on gels or used for primer extension reactions. Specific oligonucleotides (see Supplementary Table S3) were 5′-end labelled with [γ-³²P] ATP and used as probes. Hybridization signals were detected using a Typhoon™ FLA9400 imaging system (GE Healthcare) and quantified using the GelQuant.NET software (biochemlabsolutions.com).

Affinity purification of GFP-tagged proteins

GFP-tagged factors representative of 90S and pre-60S r-particles were purified following a one-step GFP-Trap_A procedure (Chromotek), as described previously (80). Lysis and purification were performed with ice-cold and low-salt GFP buffer (20 mM Tris–HCl [pH 7.5], 5 mM MgCl$_2$, 150 mM CH3COOK, 1 mM dithiothreitol [DTT], 0.2% Triton X-100), containing a protease inhibitor cocktail (Complete; Roche). The proteins from purified particles were extracted by boiling the beads with Laemmli buffer and analyzed by western blotting. To estimate that similar amounts of purified complexes are loaded on the gels, aliquots of the samples were first resolved by SDS-PAGE and visualized by silver staining.

Affinity purification of particles containing L14A-yGFP was also performed by the one-step GFP-Trap_A procedure. The pre- and mature rRNAs associated with the particles were recovered by the hot phenol-chloroform method and analysed by northern blotting as described above.

Fluorescence microscopy

To test pre-ribosomal particle export, the *GAL::RPL14* strain was transformed with plasmids expressing either GFP-tagged L25 or S3 and Nop1-mRFP (see above). Transformants were grown in selective SGal medium and shifted to selective SD for 6 h to deplete L14. Cells were washed, resuspended in PBS buffer (140 mM NaCl, 8 mM Na$_2$HPO$_4$, 1.5 mM KH$_2$PO$_4$, 2.75 mM KCl, pH 7.3), and examined with an Olympus BX61 fluorescence microscope equipped with a digital camera. Images were analysed using the Olympus cellSens software and processed with Adobe Photoshop CS2 (Adobe Systems, Inc.).

Protein extracts and western blotting analyses

Total yeast protein extracts were prepared as described previously (81). Total protein extracts and samples from purified particles were analysed by western blotting according to standard procedures. The following primary antibodies were used in this study: mouse monoclonal anti-GFP (clones 7.1 and 13.1, Roche) and anti-Nop1 (MCA28F2, EnCor Biotechnology); rabbit polyclonal anti-L1 (gift from F. Lacroute) (82), anti-L6 (gift form G, Dieci) (83), anti-L10 (gift from B. Trumpower) (84), anti-L14 (gift from G. Dieci) (83), anti-L16 (gift from S. Rospert) (85), anti-Erb1 (86), anti-Has1 (gift from P. Linder) (87), anti-Mrt4 (gift from J.P.G. Ballesta) (88). Secondary goat anti-mouse or anti-rabbit horseradish peroxidase-conjugated antibodies (Bio-Rad Laboratories, Inc.) were used as secondary antibodies. Proteins were visualized using a chemiluminescence detection kit (Super-Signal West Pico, Pierce) and a ChemiDoc™ MP imaging system (Bio-Rad Laboratories, Inc.). Images were processed with Adobe Photoshop CS2 (Adobe Systems, Inc.).

Affinity-purification of Noc2-TAP containing pre-ribosomal particles

The FEY320 strain, which expresses a chromosomally-encoded Noc2-TAP fusion protein and harbors a *GAL::HA-RPL14A* allele as the sole source of L14 r-protein, was grown in YPGal to an OD$_{660}$ of ca. 0.8 and shifted to YPD for 6–8 h to shut down *RPL14A* expression. Noc2-TAP and associated pre-ribosomal particles were then affinity purified from total cell extracts using a matrix of rabbit IgG covalently coupled to magnetic beads (Sigma-Aldrich) as described previously (19) with some minor modifications. The cell pellet corresponding to one litre of yeast culture was resuspended in 1.5 ml of cold MB buffer (20 mM Tris–HCl pH 8,0, 200 mM KCl, 5 mM (CH$_3$COO)$_2$Mg, 2 mM benzamidine, 1 mM PMSF, and 0.02 U/ml RNasin® ribonuclease inhibitor) per g of cell pellet. Cells were broken by vigorous shaking with glass beads (1.4 g beads of 0.75–1 mm diameter per 0.8 ml of cell suspension) in a Vibrax VXR shaker (IKA) for 10 min at 4°C, followed by 2 min on ice. This procedure was repeated twice. Total cell extracts were clarified by two consecutive centrifugation steps in a microfuge at the maximum speed (ca. 16 000 × *g*) for 5 min and 10 min, respectively. The protein concentration of the cleared lysated was determined using the Bradford protein assay (Bio-Rad). To each of the resulting supernatants (typically 1 ml with ca. 50 mg of total protein), Triton X-100 (0.5% final), Tween 20 (0.1% final) and 200 μl of IgG-coupled magnetic beads slurry, equilibrated with MB buffer containing 0.5% Triton X-100 and 0.1% Tween, were added, and the mixture was incubated for 2 h 30 min at 4°C with end-over-end tube rotation. After incubation, the beads were washed four times with 700 μl cold MB buffer with 0.5% Triton X-100 and 0.1% Tween 20. RNA was extracted from the 20% of the mixture to perform northern blot analyses.

The remaining 80% mixture was washed two times with 1 ml AC buffer (100 mM CH_3COONH_4, pH 7.4, 0.1 mM $MgCl_2$) to remove excess of salt from the samples and bound proteins eluted two times with 500 μl of freshly prepared 500 mM NH_4OH solution for 20 min at room temperature, pooled and lyophilized over night.

Semiquantitative mass spectrometric analyses

Lyophilized eluates were further processed for iTRAQ (isobaric tags for relative and absolute quantitation) and mass spectrometric protein analyses, as exactly described (89). Proteins identified by only one peptide were discarded. iTRAQ ratios (depleted versus non-depleted sample) were determined and normalized to the ratio of the Noc2 bait protein.

RESULTS

Yeast L14 assembles in the nucle(ol)us within early pre-60S r-particles

Assembly of most r-proteins occurs primarily in the nucle(ol)us, although few ones appear to load preferentially or exclusively in the cytoplasm (reviewed in (9)). No specific information was available on the course of the incorporation of yeast L14 into pre-60S r-particles. Despite the fact that no nuclear localization sequence can apparently be predicted for L14 (cNLS mapper programme, (90); NucPred tool, (91)), assembly of L14 is expected to occur in the nucleus. Indeed, Milkereit *et al.* have shown that L14 is included in the broad list of r-proteins that are roughly equally enriched in early to late pre-60S r-particles (19). Consistently, L14 has been identified at its final location in cryo-EM maps of distinct nuclear pre-60S r-particles (e.g. (44,45,51)).

To explore in further detail the timing of incorporation of L14 into pre-60S r-particles, we first monitored the localization of an L14A-yGFP construct upon induction of dominant negative *NMD3-Δ100* allele, which has been proven to trap nascent pre-60S r-particles in the nucleus (92). The L14A-yGFP construct fully complemented the growth and ribosome biogenesis defects of the null *rpl14AΔ rpl14BΔ* strain (Supplementary Figure S3). As shown in Supplementary Figure S4, L14A-yGFP accumulated in the nucleus of most of the cells examined upon overexpression of the Nmd3-Δ100 protein, but it was found in the cytoplasm under non-inducible conditions. No changes in the cytoplasmic distribution of L14A-yGFP was observed upon overexpression of a wild-type Nmd3 protein (data not shown).

Next, we tested for the presence of L14 within different affinity-purified pre-ribosomal particles, via GFP-tagged assembly factors, along the road of pre-60S particle maturation. The specificity of the purification was evaluated by assessing the presence of the selected *trans*-acting factors Nop1, Erb1, Has1 and Mrt4 by western blot using specific antibodies (Figure 1). Western blot analyses also showed that L16 significantly co-enriched with practically all tested pre-60S particles (Figure 1; see also (81)), as did L1, which was used as a control of an early assembling r-protein (19,32). In contrast, L10, which has been reported to assemble in the cytoplasm (19,93), only co-enriched
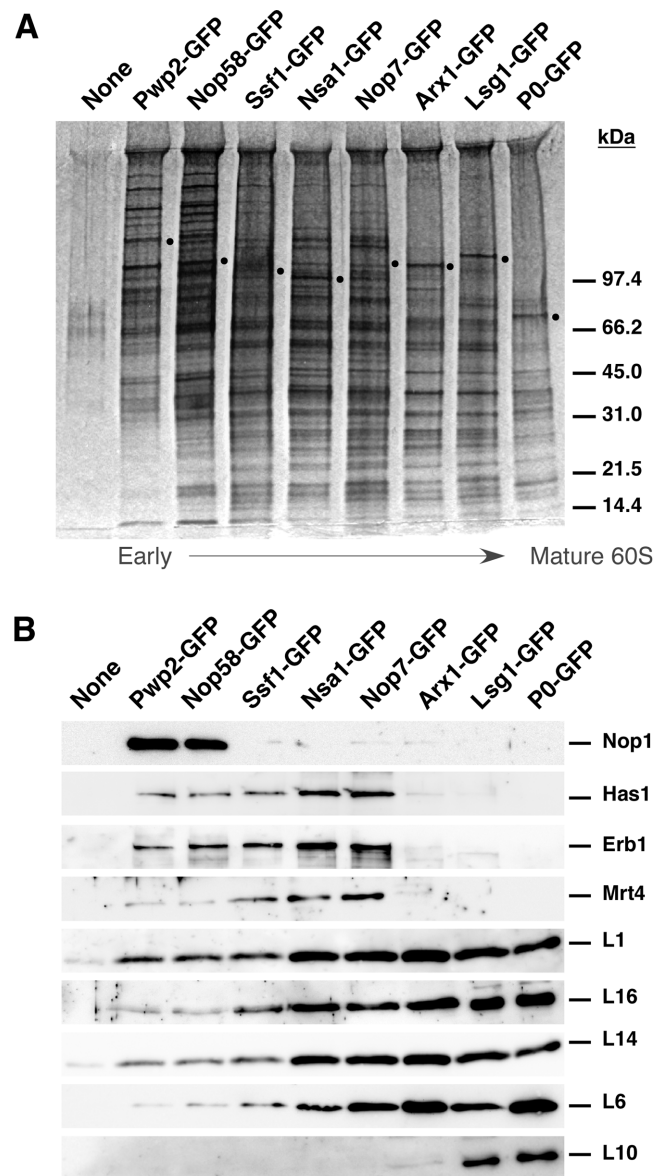
Figure 1. Association of L14 with maturing 60S r-subunits. 90S and pre-60S r-particles from early to late intermediates were affinity-purified by using the GFP-Trap® immunoprecipitation procedure with the indicated bait proteins. Equivalent amounts of immunoprecipitates were separated by 12% SDS-PAGE and subjected to silver staining (**A**) or western blot analysis (**B**). Specific antibodies were used to detect the Nop1, Has1, Erb1 and Mrt4 *trans*-acting factors and the L1, L6, L10, L14 and L16 r-proteins. Dots indicate the positions of bait proteins. Pre-ribosomal particles are ordered along the 60S r-subunit assembly pathway.

with late and cytoplasmic pre-60S r-particles and P0-GFP-containing particles that correspond mainly to mature ribosomes (33). Interestingly, neither L14 nor L16 seemed to be as stably associated with early 90S particles, which were purified using GFP-tagged Pwp2/Utp1, as L1 (see Discussion); similar results to those of L14 were obtained for L6, a r-protein that directly interacts with L14 (41,43), which we found even poorer represented in early 90S/66S particles purified using GFP-tagged Nop58/Nop5 than L14 (Figure
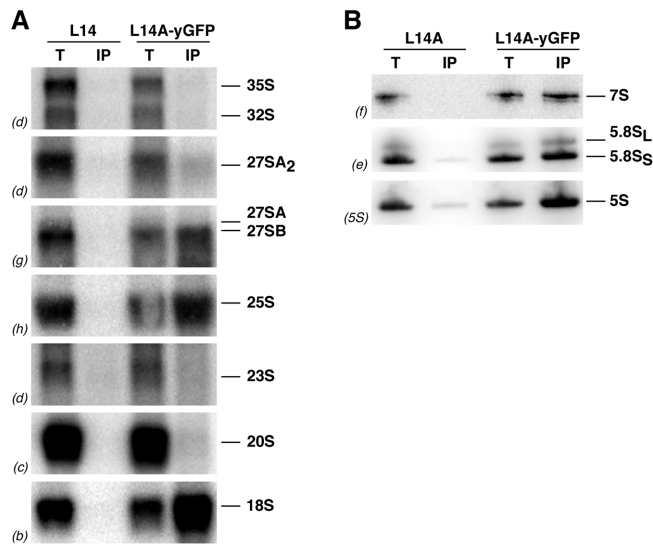
Figure 2. L14-yGFP stably assembles with pre-60S r-particles containing 27SB pre-rRNAs. Affinity-purification of ribosomal particles was performed from cells expressing L14A-yGFP *via* the GFP-Trap® immunoprecipitation procedure. Wild-type cells (untagged L14) were used as a negative control. Total RNA was extracted from whole cell extracts (T) and immunoprecipitates (IP) and analysed by northern blotting. (**A**) Northern blot analysis of high-molecular-mass or (**B**) low-molecular-mass pre- and mature rRNAs. The indicated probes, between parentheses, were used to detect the different pre- and mature rRNA species (see Supplementary Figure S1A and Supplementary Table S3).

1). Together, these data indicate that L14 assembles into early nucle(ol)ar pre-60S r-particles.

In agreement with these results, when we affinity purified L14A-yGFP-containing particles and assayed those pre-rRNA intermediates that co-purified by northern blot hybridization, we detected 27SB and 7S pre-rRNAs clearly above background levels (Figure 2). As expected for an r-protein (31,37,74), there was a significant co-purification of mature rRNAs with L14A-yGFP (Figure 2). The 27SA$_2$ pre-rRNA was also detected, albeit only slightly above background levels (Figure 2), suggesting that either L14A associates with pre-60S r-particles once cleavage at site A$_2$ has occurred or more likely that the assembly of L14 is only stabilized after some reorganization of the pre-rRNAs that takes place concomitantly to the formation of 27SB pre-rRNAs. Taken together, all these results suggest that L14 assembles into early pre-60S r-particles and appears to become stably associated only with those containing the 27SB pre-rRNAs.

## L14 is required for normal accumulation of 60S ribosomal subunits

L14, as most r-proteins (e.g. (94)), is essential for cell viability, and is encoded by two different paralogous genes, *RPL14A* and *RPL14B*. Deletion of *RPL14A* caused a severe defect on growth, while deletion of *RPL14B* led to a minor growth defect (Supplementary Figure S5A, see also (71,94)). These defects seemed to be exacerbated at lower temperatures (Supplementary Figure S5A). As shown in Supplementary Figure S5B, both deletions led to polysome profiles alike to those for mutants showing a deficit in the

content of 60S r-subunits. Thus, for the profiles of both deletion strains, we observed a decrease in the amount of free 60S r-subunits relative to free 40S r-subunits and the appearance of half-mer polysomes. The overall defects were apparently more pronounced for the *rpl14A∆* than for the *rpl14B∆* null strain. These data are in agreement with those previously described in a previous report (71).

For the phenotypic analysis of the complete loss-of-function of L14, we constructed a conditional strain, named *GAL::RPL14* strain, that expressed a double HA-tagged variant of L14A as the sole cellular source of L14 under the control of a *GAL* promoter. This strain grew as the isogenic wild-type strain or a isogenic *RPL14* control strain on YPGal plates, but was unable to grow on YPD plates (Figure 3A). After shifting a culture of the *GAL::RPL14* strain from liquid YPGal to YPD medium, the rate of cell division slowed down significantly in few hours and practically stopped after 8–10 h in YPD (data not shown). When we analysed polysome profiles from cell extracts of the *GAL::RPL14* strain grown in YPGal, normal wild-type profiles were obtained (Figure 3B). However, when shifted for ∼3 h to YPD, extracts showed abnormal polysome profiles, consisting of a clear decrease in the levels of free 60S versus free 40S r-subunits, a decrease in the 80S peak and polysomes and the appearance of half-mer polysomes (Figure 3B). Taken together, these results indicate that L14 is essential for growth and for normal accumulation of 60S r-subunits.

L14 is required for 27S pre-rRNA processing and normal production of 25S and 5.8S rRNAs

To study whether the deficit of 60S r-subunits caused by the depletion of L14 is attributed to a defective production or/and an excessive degradation of 60S r-subunits, we analysed the effects of L14 depletion on the synthesis and processing of pre-rRNAs by [^{3}H]uracil pulse-chase labelling experiments. For this purpose, the *GAL::RPL14* and an isogenic wild-type control strain were grown in SGal-Ura and shifted to SD-Ura for 6 h. In wild-type cells, the 35S pre-rRNA was processed rapidly into 32S pre-rRNA and then into 27S and 20S pre-rRNAs, which were subsequently converted into mature 25S, 5.8S and 18S rRNAs, respectively (Figure 4). In contrast, in the *GAL::RPL14* strain, processing of the 35S pre-rRNA was delayed; as a consequence, less 27SA and 20S pre-rRNAs were formed and traces of 23S pre-rRNA were detected, but while enough mature 18S rRNA was still made, some 27S pre-rRNAs persisted even after the 60 min of chase and practically no labelled mature 25S and 5.8S rRNAs were detected (Figure 4). These defects were apparently specific since no changes in the kinetics of production of mature 5S rRNA or tRNAs were observed upon the depletion of L14 (Figure 4). These results indicate that the deficit in 60S r-subunits following depletion of L14 was due to impaired processing and increased turnover of 27S pre-rRNAs. As a consequence, reduced levels of both mature 25S and 5.8S rRNAs were synthesized. Most likely as a side effect (for further discussion, see (81) and references therein), earlier processing reactions at sites A$_0$, A$_1$ and A$_2$ were also delayed upon depletion of L14; however,
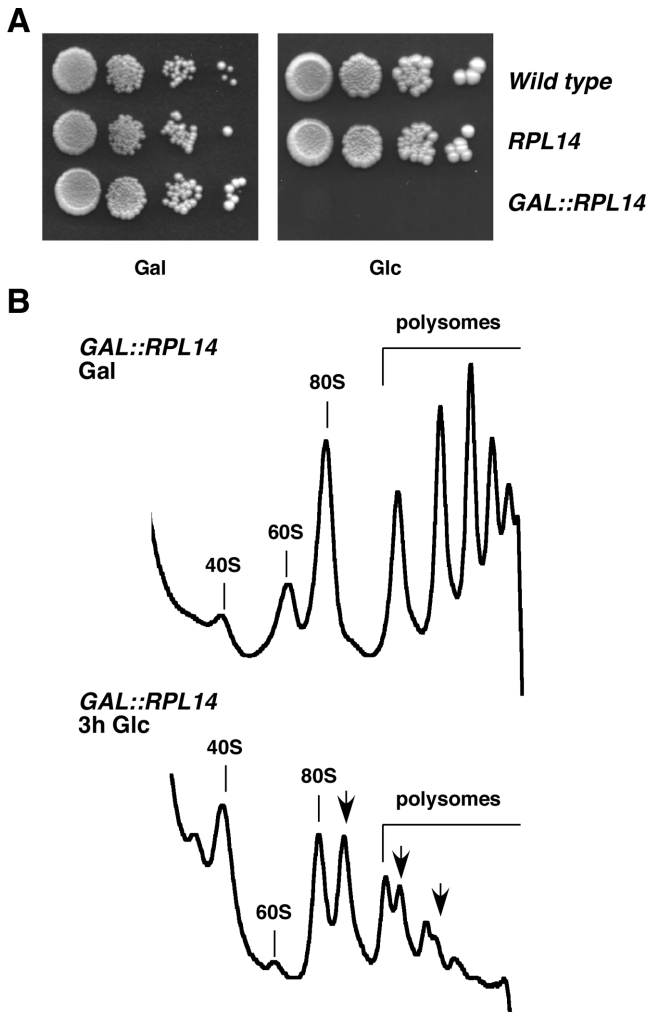
Figure 3. Depletion of L14 results in a deficit in 60S r-subunits. (**A**) Growth comparison of the strains W303–1B (*Wild type*), FEY229 [YCplac111-RPL14A] (*RPL14*) and FEY229 [pAS24-RPL14A] (*GAL::RPL14*). The cells were grown in YPGal and diluted to an OD_{600} of 0.05. A 5-fold series of dilutions were performed and 5 μl drops were spotted onto YPGal (Gal) and YPD (Glc) plates. Plates were incubated at 30°C for 3 days. (**B**) Polysomes profile analysis of *GAL::RPL14* cells grown in YPGal (Gal) or shifted to YPD (Glc) for 3 h. Cells were harvested at an OD_{600} of ∼0.8, whole cell extracts were prepared and 10 A_{260} units of each extract were resolved in 7–50% sucrose gradients. The A_{254} was continuously measured. Sedimentation is from *left* to *right*. The peaks of free 40S and 60S r-subunits, 80S vacant ribosomes or monosomes and polysomes are indicated. Half-mers are labelled by arrows.

this delay had only a slight impact on 18S rRNA production.

Depletion of L14 affects negatively 27S pre-rRNA processing

To define the exact pre-rRNA processing steps that are affected upon depletion of L14, we evaluated changes in the steady-state levels of mature rRNA and pre-rRNA intermediates. For this purpose, total RNA was isolated from the *GAL::RPL14* and an isogenic wild-type control strain grown in YPGal or at various time points after a shift to YPD and analysed by northern blotting and primer extension.
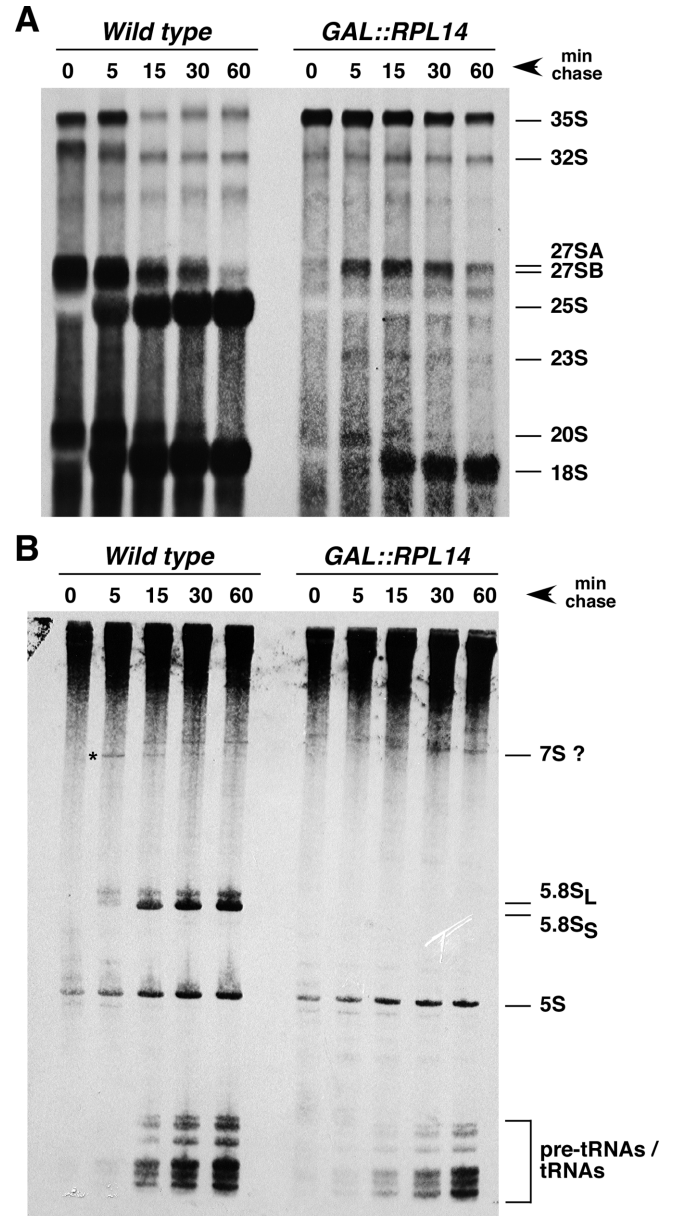
Figure 4. Depletion of L14 impairs 27S pre-rRNA processing. (**A**) Wild-type strain W303–1B (*Wild type*) and FEY229 [pAS24-RPL14A] (*GAL::RPL14*) were transformed with YCplac33 (*CEN URA3*), grown at 30°C in SGal-Ura to mid log phase and shifted to SD-Ura for 6 h. Cells were pulse-labelled with [5,6-^{3}H]uracil for 2 min followed by a chase with a large excess of unlabelled uracil for the times indicated. Total RNA was extracted from each sample and 20,000 cpm was loaded and separated on (**A**) a 1.2% agarose-6% formaldehyde gel or (**B**) a 7% polyacrylamide-8M urea gel, transferred to nylon membranes and visualized by fluorography. The positions of the different pre- and mature rRNAs are indicated. We suppose that 7S pre-rRNA corresponds to the species labelled with an asterisk, which only appears in the wild-type condition.

As shown in Figure 5A, and consistent with the pulse-chase data, depletion of L14 resulted in a minor decrease in 18S rRNA and in a more drastic decrease in 25S rRNA. Slight changes in the levels of different pre-rRNAs were observed for the wild-type strain grown in YPGal or shifted to YPD, which are most likely due to the effects of the nutri-
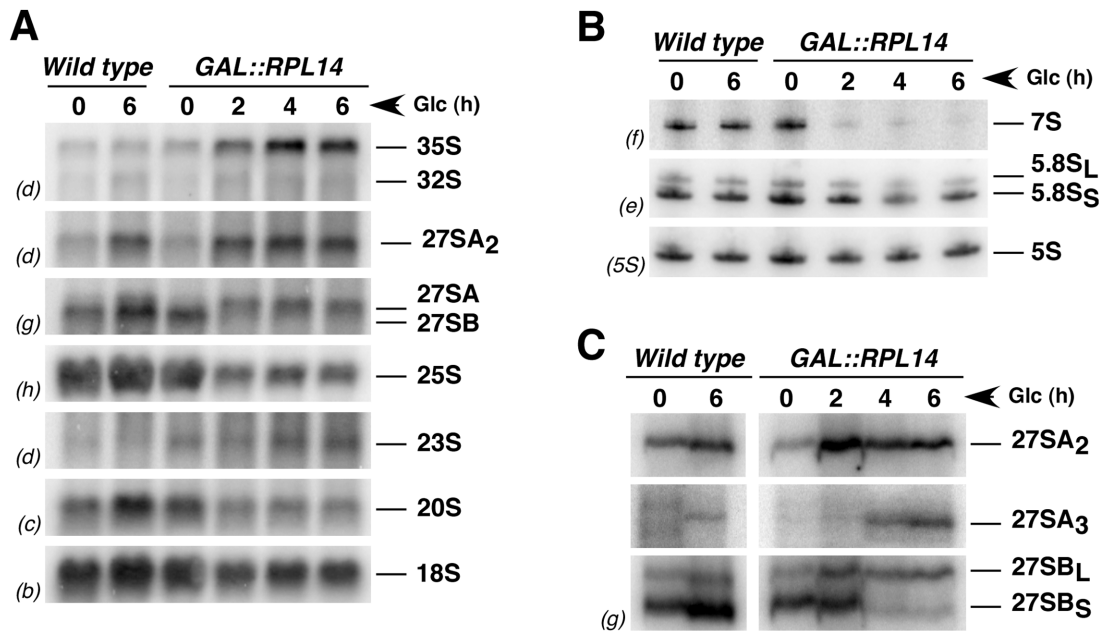
Figure 5. Depletion of L14 affects the steady-state levels of pre-rRNA and mature rRNA species. Strains W303–1B (*Wild type*) and FEY229 [pAS24-RPL14A] (*GAL::RPL14*) were grown at 30°C in liquid YPGal medium and shifted to YPD. Total RNA was extracted from the cultures at the indicated times after the shift and equal amounts (5 μg) were subjected to northern hybridization or primer extension analysis. (**A**) Northern blot analysis of high-molecular-mass or (**B**) low-molecular-mass pre- and mature rRNAs. Probes, between parentheses, are described in the Supplementary Figure S1A and Supplementary Table S2. (**c**) Primer extension analysis with probe g, which is complementary to sequences in ITS2 (Supplementary Figure S1A). This probe allows detection of 27SA$_2$, 27SA$_3$ and both 27SB pre-rRNAs.

tional up-shift from the galactose- to the glucose-containing medium (95). More significant differences were observed for the *GAL::RPL14* strain, thus, 35S and aberrant 23S pre-rRNAs progressively accumulated with ongoing depletion of L14. However, while levels of 20S pre-rRNA mildly decreased, those of 27SA$_2$ pre-rRNA initially accumulated but, then, remained apparently unaffected 6 h after transfer to YPD. In contrast, the levels of 27SB pre-rRNAs clearly decreased. Analysis of low-molecular-weight rRNAs revealed a significant decrease in the steady-state levels of 7S pre-rRNAs, a slight reduction in those of mature 5.8S rRNAs, but no alteration in the levels of 5S rRNA in the L14-depleted strain (Figure 5B). Importantly, the ratio of 5.8S$_L$ *versus* 5.8S$_S$ rRNA was not affected by the depletion of L14.

We also performed primer extension assays to identify 27SA$_3$ pre-rRNA and to distinguish between 27SB$_L$ and 27SB$_S$ pre-rRNAs. As shown in Figure 5C, primer extension did not shown any differences in the levels of 27SA$_2$ pre-rRNA, fully consistent with the results obtained by northern hybridization. However, a clear but mild accumulation of 27SA$_3$ pre-rRNA was observed upon depletion of L14. Moreover, we could also observe a slight accumulation of 27SB$_L$ pre-rRNA and a significant reduction in 27SB$_S$ pre-rRNA levels with ongoing depletion of L14. Altogether, these results indicate that L14 is required for processing of 27SA$_2$ and 27SA$_3$ pre-rRNAs to 27SB pre-rRNA species. In addition, the presence of L14 in pre-60S r-particles is needed for the stability of 27SB precursors. Thus, although 27SB$_L$ pre-rRNA is still made in L14-depleted cells, it fails to be converted to 7S$_L$ pre-rRNA and is consequently de-

graded. In these circumstances, the 27SB$_S$ pre-rRNA is even less stable than the 27SB$_L$ pre-rRNA and, therefore, it could neither be converted into its subsequent 7S$_S$ pre-rRNA.

Depletion of L14 leads to nuclear retention of pre-60S ribosomal particles

Among the distinct phenotypes of most loss-of-function mutants in 60S r-subunit assembly factors and/or 60S r-proteins that lead to an impairment of pre-rRNA processing is the failure in nuclear export of pre-60S r-particles (e.g. (31,38,96)). Thus, to test whether depletion of L14 impairs 60S r-subunit export, we studied the localization of a GFP-tagged L25 r-protein upon depletion of L14. The use of the L25-eGFP reporter to trace the nucleo-cytoplasmic transport of 60S r-subunits by fluorescence microscopy has been well established (37,80,97). As shown in Figure 6, and as expected for an r-protein, a predominantly cytoplasmic distribution of L25-eGFP with vacuolar and nuclear exclusion was observed in *GAL::RPL14* cells grown to early log phase in selective SGal medium. However, *GAL::RPL14* cells shifted to selective SD medium exhibited an accumulation of the reporter in the nucleus, as denoted by its colocalization with the red fluorescently tagged Nop1 marker. In many cells, the GFP-decorated region mostly coincided with the RFP-decorated one, thus, indicating that L25-eGFP mainly accumulated in the nucleolus. We did neither observe nuclear accumulation of 40S r-subunit reporter S3-eGFP upon depletion of L14 nor of L25-eGFP when the isogenic wild-type control strain was grown in selective SD medium (data not shown). Taken together, these results indicate that intranuclear transport from the nucleolus to the
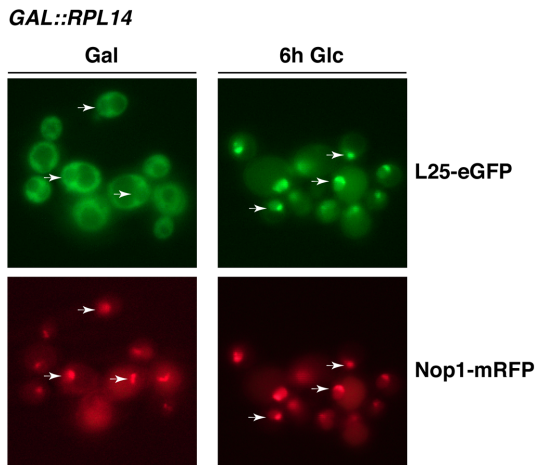
Figure 6. Depletion of L14 results in retention of pre-60S r-subunits in the nucle(ol)us. FEY229 [pAS24-RPL14A] (*GAL::RPL14*) cells co-expressing the nucleolar Nop1-mRFP and the 60S r-subunit reporter L25-eGFP were grown in SGal-Trp (Gal) or shifted to SD-Trp up to 6 h. The subcellular localization of the r-protein L25-eGFP and the NOP1-mRFP marker was analysed by fluorescence microscopy. Arrows point to nucleolar fluorescence. Approximately 200 cells were examined for each reporter, and practically all cells gave the results shown in the pictures.

nucleoplasm, as well as nucleocytoplasmic export of pre-60S r-particles are blocked upon depletion of L14.

L14 is required for the stable assembly of 60S r-proteins located at its immediate neighborhood and surrounding the polypeptide exit tunnel

To further study the role of L14 in 60S r-subunit biogenesis, we determined how the depletion of L14 affected the assembly of other 60S r-proteins with pre-60S r-particles. For this purpose, we chromosomally TAP-tagged Noc2 in the *GAL::RPL14* strain, affinity purified TAP-tagged Noc2-containing pre-ribosomal particles in the presence of L14 or upon its depletion, and compared the rRNA and protein composition in both conditions. Noc2 is an early pre-60S assembly factor that is present in early to intermediate pre-60S r-particles, but apparently weakly associated with 90S pre-ribosomal particles, and dissociates from particles before or concomitant to 27SB pre-rRNA processing at site C_2 (19,98,99). Our analysis indicates that the depletion of L14 does not impair the recruitment of Noc2-TAP to pre-ribosomal particles; thus, before or after depletion of L14, Noc2-TAP co-purified early to intermediate pre-60S r-particles. The pre-rRNA content of these complexes was consistent with the relative abundance of the same pre-rRNAs in the total cell extracts of the L14-depleted or undepleted control cells; thus, increased co-purification of 35S and 27S pre-rRNAs with Noc2-TAP was observed upon depletion of L14, while significant co-purification of 27S pre-rRNAs was observed for undepleted control cells (Supplementary Figure S6). We also compared changes in protein composition of TAP-tagged Noc2-containing particles purified from L14-depleted versus L14-undepleted cells focusing first on the category of r-proteins. As shown in Figure 7A, and as expected, L14 itself was the r-protein whose levels were most severely diminished. The levels of about

a dozen other r-proteins were also mildly but significantly reduced upon depletion of L14. These proteins can be classified into different groups: (i) L6, L16, L20 and L33, which all belong to the neighborhood area of L14. L14 directly interacts with the r-proteins L6, L9, L16 and L20 (43), but while L6 and L20 appeared substantially underrepresented, L9 could not be detected in our analysis and, strikingly, L16 was only very marginally affected upon depletion of L14 (see Discussion). All these r-proteins are involved in early steps of 60S r-subunit assembly and their respective depletion leads to practically identical pre-rRNA processing defects to those we have described for the depletion of L14 (21,38,100). (ii) L17, L19, L26, L37 and L39, which are all located around the polypeptide exit tunnel or its nearby region (43). All these are middle-acting r-proteins required for 27SB pre-rRNA processing ((31,37,38,74) and our unpublished results). (iii) A miscellaneous group composed of L1 (uL1), L2, L28 (uL15), L34 (eL34) and L36 (eL36). Remarkably, L28 and L36 interact directly with each other in the mature 60S r-subunit (43), and L34 and L36 form part of the same functional network of the *trans*-acting factor Ebp2 (101). Depletion of L36 leads to practically identical pre-rRNA processing defects as depletion of L14 (101). In turn, L34 is required for 27SB pre-rRNA processing (38). (iv) L10 and L24, which, as mentioned above, assemble in the cytoplasm (9). Decreased representation of these two r-proteins upon depletion of L14 could likely be the artifactual result of some minor mature 60S r-subunit contamination after Noc2-TAP purification from L14-undepleted extracts.

In turn, the levels of several other r-proteins significantly increased in Noc2-TAP purified complexes upon depletion of L14. These include many early-acting r-proteins such as L3, L7, L8, L13, L15, L18 or L32, the r-proteins components of the 5S rRNP (L5 and L11), and the r-stalk protein P0 (uL10) and its base L12 (uL11). Likely, these proteins either assemble earlier than L14 into pre-60S r-particles (i.e. L3), thus, not being affected by the depletion of L14, or belong to ribosomal modules whose assembly occurs regardless of the presence or the absence of L14 in pre-ribosomal particles.

Together, these results indicate that L14 contributes to the optimal formation of an early pre-ribosomal structure that comprises mostly those r-proteins located at the central solvent interface of 60S r-subunits and the adjacent region surrounding the polypeptide exit (see Supplementary Figure S7). All these r-proteins are either involved in $27SA_2$ and $27SA_3$ pre-rRNA processing reactions as L14 or in the immediately downstream step of 27SB pre-rRNA processing.

L14 is required for the stable association of a set of 60S r-subunit biogenesis factors required for processing of 27SB pre-rRNA

We also determined how the depletion of L14 affected the association of *trans*-acting factors with Noc2-TAP affinity-purified pre-ribosomal particles. Notably, relatively few factors showed reduced association, albeit to significantly different extents, allowing their classification into two groups of differentially diminished factors (Figure 7B). Most of
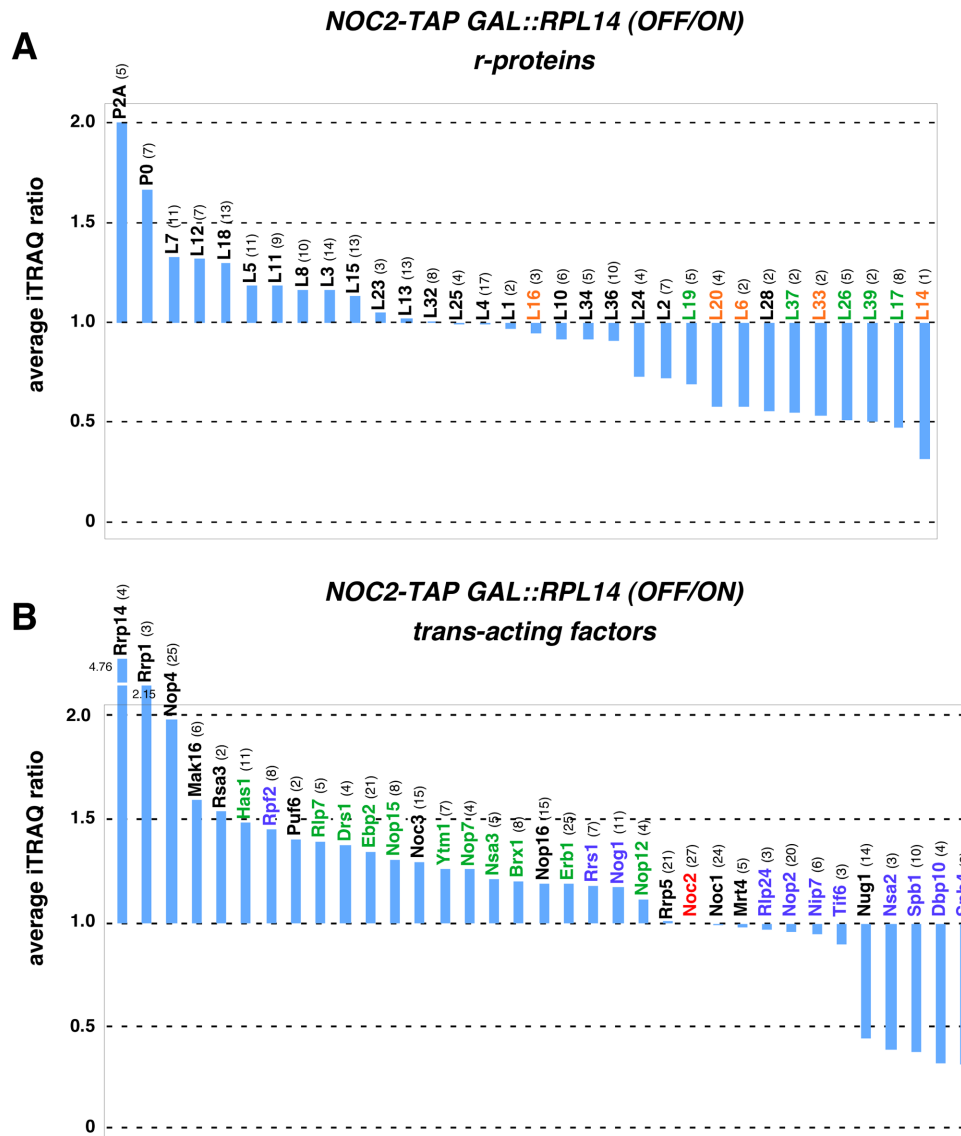
Figure 7. Changes in composition of pre-ribosomal particles upon depletion of L14. Strain FEY320, which expresses a genomic *NOC2-TAP* allele from its cognate promoter and harbors a plasmid-borne *HA-RPL14A* allele driven by the *GAL1–10* promoter, was cultivated at 30°C in YPGal and shifted to YPD for 6 h to shut down the expression of L14. Whole cell extracts were prepared for each condition, complexes associated with Noc2-TAP affinity purified and the co-purifying proteins processed for comparative protein analysis by semiquantitative mass spectrometry using iTRAQ (see Material and Methods). The mean of two independent experiments is shown. Average iTRAQ ratios of all respective proteins identified by more than one peptide are indicated. Numbers in parentheses indicate the number of peptides by which the respective protein was identified. (**A**) Relative enrichment/deprivation of r-proteins purified upon depletion of L14. L14 and its neighboring r-proteins in the mature 60S r-subunits are marked in orange; r-proteins that surround the nascent polypeptide exit tunnel are marked in green (**B**) Relative enrichment/deprivation of *trans*-acting factors purified upon depletion of L14. Noc2, whose ratio was set to one, is marked in red; A$_3$ factors are marked in green; B factors are marked in light blue.

these factors (also known as B-factors), Spb4, Dbp10, Spb1, Nsa2, Tif6, Nip7, Nop2 and Rlp24, are required for 27SB pre-rRNA processing, thus for cleavage at site C$_2$ within ITS2 (102–110). Remarkably, Sbp4, Dbp10, Spb1 and Nsa2 are more strongly and similarly reduced, while there is only a modest decrease in Tif6, Nip7, Nop2 and Rlp24 (Figure 7B). Dbp10, Tif6, Rlp24 are among the subset of factors required to recruit Nsa2 to pre-60S r-particles (102) and Nip7 and Nop2 form a heterodimer (102). Nug1, which is apparently not a B-factor, also significantly decreased (Figure 7B). It has been shown that Nug1 genetically interacts with and is required for the stable association of Dbp10 with pre-ribosomal particles (111,112).

Few other factors required for 27SB pre-rRNA processing are enriched upon depletion of L14, among them Nog1 and the Rpf2-Rrs1 heterodimer (59), which guides assembly of the 5S rRNP (see (58), and references therein). The significance of the enrichment of Rrp14, Nop4, Nop16, Rsa3, Puf6 and Noc3 is still unclear (but see Discussion), although it has been described that Rrp14 delays 27SB pre-rRNA processing and interacts with Ebp2 in a two-hybrid assay (113). Remarkably, practically all A$_3$-factors so far described were found among the proteins that were enriched

upon depletion of L14: Has1, Drs1, Rrp1, Nop12, Brx1, Ebp2, Nop7, Ytm1, Erb1, Nsa3/Cic1, Nop15 and Rlp7 (for details, see (10)). Depletion of any of these factors leads to a defect in 27SA$_3$ pre-rRNA processing (e.g. (114)), a phenotype that it is the most significant feature of L14 depletion (see Figure 5C). It has been shown that factors Nop7, Ytm1 and Erb1 form a stable sub-complex with which Drs1 associates (115,116). This sub-complex together with Nsa3, Nop15 and Rlp7 has been described to be mutually interdependent for association with pre-60S r-particles (114). Has1 interacts with Nop15 in a two-hybrid assay (117).

In conclusion, depletion of L14 prevents stable association of a set of factors required for 27SB pre-rRNA processing with early pre-60S r-particles. Consequently, these particles are unable to progress in their maturation at ITS2 of the pre-rRNAs. In contrast, these particles remain associated with most factors required for 27SA$_3$ pre-rRNA processing, but strikingly they are also unable to support this pre-rRNA processing reaction, as evidenced by the pre-rRNA processing defects observed upon L14 depletion. Likely as the direct consequence of these impairments, early pre-60S r-particles are subjected to nuclear retention and efficient turnover following depletion of L14.

Importance of the eukaryote-specific C-terminal extension of L14 in 60S r-subunit biogenesis and function

In both pre-60S r-particles and mature 60S r-subunits, an interaction between the most distal α-helices of the eukaryote-specific C-terminal extensions of L14 and L16 is observed (43,44,51) (see also Supplementary Figures S8 and S18). This interaction is maintained by apolar contacts between amino acids of both extensions and two salt bridges, one between the carboxylic group of L14[A138] and the ε-amino group of L16[K177] and another between the guanidinium group of L14[R109] and the carboxylic group of L16[Y199] (81) (see also Supplementary Figure S8). To study the relevance of this interaction for cell growth, ribosome biogenesis and function, we performed several analyses:

(i) We first examined the effect of stepwise truncation of the C-terminal extension of L14 on cell viability, in a similar way as previously done for the C-terminal extension of L16 (81,100). The truncations were designed to eliminate only one or the two distal C-terminal α-helices of L14 involved in the interaction with the C-terminal extension of L16 in the 60S r-subunit (see Supplementary Figures S8 and S9A). Then, we transformed a *RPL14* shuffle strain with YCplac111 centromeric plasmids harboring either full-length *RPL14A* or three serial *rpl14A* truncation alleles under the control of the cognate *RPL14A* promoter. Transformed cells were restreaked on selective SD-Leu plates and subjected to plasmid shuffling on 5-fluoroorotic acid (5-FOA)-containing plates. As expected (71), expression of the wild-type L14A or the truncated L14A-N122 protein variant (previously termed L14A-L123* (71)) sustained cell growth as the sole source of L14 in the cells. However, expression of the truncated protein variants lacking completely the more distal C-terminal α-helix (L14A-N109 construct)
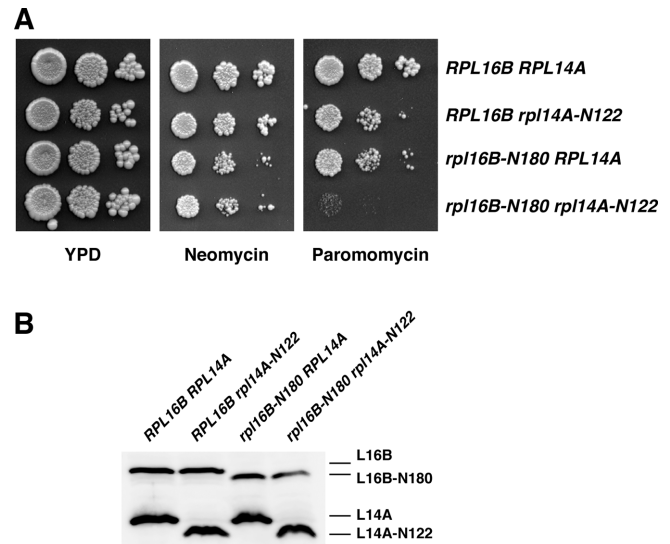
Figure 8. The *rpl14A-N122 rpl16B-N180* mutant is hypersensitive to paromomycin. (**A**) Growth phenotypes of the indicated strains on YPD plates without antibiotics or containing 5 mg/ml neomycin or 1 mg/ml paromomycin. A triple *rpl14AΔ rpl14BΔ rpl16AΔ* null mutant containing the indicated combinations of plasmid-borne *RPL14A* or *rpl14A-N122* alleles with chromosomal *RPL16B* or *rpl16B-N180* alleles as sole sources of L14 and L16, respectively, were grown in YPD medium and spotted in 10-fold serial dilution steps onto YPD plates with or without the indicated antibiotics. Plates were incubated at 30°C for 3 days. (**B**) Expression levels of the plasmid-borne wild-type and indicated mutant alleles of both *RPL14A* and *RPL16B* genes as sole cellular source of L14 and L16 r-proteins. Equivalent amounts of cell extracts of the above strains were separated by SDS-PAGE and levels of the L14 and L16 r-proteins variants were determined by western blot analysis using specific anti-L14 and anti-L16 antibodies.

or the last two C-terminal α-helices of L14 (L14A-N97 construct) did not support growth (Supplementary Figure S9B).

(ii) We also tested the genetic interaction between the viable *rpl14A-N122 rpl14BΔ* mutant and the previously reported viable *rpl16AΔ rpl16B-N180* mutant, which expresses a truncated L16B variant lacking the last 18 amino acids, as the sole source of L16 (81). The *rpl14A-N122* and *rpl16B-N180* alleles, when expressed as the sole copy of each respective r-protein in yeast cells, confer a practically wild-type phenotype at 30°C and a mild 60S r-subunit deficit (71,81) (see also Figure 8A and Supplementary Figure S10). Moreover, combination of these two alleles as the sole sources of L14 and L16 in mutant cells did not cause any synergistic growth defect in either rich or synthetic media at either 30°C, 37°C or 22°C (Figure 8A and data not shown), and both protein variants were expressed to wild-type levels (Figure 8B). In agreement with the absence of defects in growth, the *rpl14A-N122 rpl16B-N180* mutant did not lead to increased 60S r-subunit shortage (Supplementary Figure S10) or stronger impairment of pre-rRNA processing (Supplementary Figure S11) than either of its parental *rpl14A-N122 rpl14BΔ* or *rpl16AΔ rpl16B-N180* mutants. Interestingly, the *rpl14A-N122 rpl16B-N180* mutant, but neither of its parental strains, displayed increased sensitivity to paramomycin (Fig-

ure [8]A). This observation suggests that, despite their practically wild-type growth rate at 30°C, cells lacking the most distal parts of the C-terminal extensions of L14 and L16 produce 60S r-subunits that might have some structural alterations and therefore manifest slight dysfunctions when subjected to certain stresses, such as the presence of distinct antibiotics that inhibit translation.

(iii) It has been shown that L14 genetically interacts with the *trans*-acting factors Mak5, Ebp2 and Nop16. Indeed, a combination of an *rpl14A-N122 RPL14B* strain with either a *mak5-N723* or an *ebp2-N286* strain resulted in a strong synthetic enhancement phenotype of the respective double mutants, while its combination with a *nop16Δ* null allele only weakly impaired the growth of the corresponding double mutant ([71]). To expand these previous observations to mutant alleles of the genes coding for the closest neighbors of L14, the L6 and L16 proteins, we tested the synthetic interaction relationship between either an *rpl16AΔ rpl16B-N180* or a *rpl6AΔ RPL6B* mutant and the same alleles of the abovementioned *trans*-acting factors. Moreover, to better compare the results obtained, we re-examined the same genetic interactions with an *rpl14A-N122 rpl14BΔ* strain where the sole source of L14 was the truncated L14A-N122 variant protein. As shown in Supplementary Figure S12, the *rpl14BΔ* allele synthetically enhanced the reported mild growth defect of the analysed *mak5*, *ebp2* and *nop16Δ* mutant alleles. Most importantly, the *rpl14A-N122 rpl14BΔ* mutant showed a synthetically lethal interaction with these *mak5*, *ebp2* and *nop16Δ* mutant alleles. Regarding the *rpl16AΔ rpl16B-N180* mutant, clear synthetic enhancement interactions were detected with the *mak5-N723*, m*ak5-N727* and *ebp2-N286* alleles, while no apparent genetic interaction was observed with the *mak5*[G218D] mutation or the null *nop16Δ* allele (Supplementary Figure S13). Strikingly, the strength of these interactions perfectly matches those previously detected for the *rpl14A-N122 RPL14B* mutant with those *mak5*, *ebp2* and *nop16Δ* mutant alleles ([71]). In contrast, any combination of those mutations with the *rpl6AΔ RPL6B* strain did not lead to synthetic enhancement phenotypes (Supplementary Figure S14). Altogether, the otherwise specific genetic interactions described above strongly suggest a functional dependence of selected components of the so-called Mak5 cluster factors, specially Mak5 and Ebp2, for the assembly of L14 and L16 r-proteins into early pre-60S r-particles, our results envisaging crucial roles of the C-terminal extensions of these two r-proteins during their stable assembly.

DISCUSSION

Significant insight into the contribution of 60S r-proteins to ribosome biogenesis has been obtained during the last years (see ([9]) and references therein). Nonetheless, few orphan 60S r-proteins, especially non-essential ones, still await characterization. In this work, we have undertaken the functional analysis of yeast L14 in ribosome synthesis. L14 is an essential protein found in eukaryotic ribosomes and in

some, but not all, archaeal ribosomes; eukaryotic L14 contains, however, a specific C-terminal extension, which is absent in the archaeal orthologs ([70],[71]).

In this work, we have addressed the timing of L14 assembly using different complementary approaches and demonstrated, as initially expected (e.g. ([19],[44])), that L14 assembles in the nucle(ol)us with pre-60S r-particles. Interestingly, our affinity purification analyses of ribosomal particles using the GFP-Trap technique indicated that L14 stably assembles into early pre-60S r-particles that contain 27SB pre-rRNA, similarly as other r-proteins such as L7 ([118]), L16 (our unpublished results), L17 ([37]), L26 ([74]) and L37 ([37]). In agreement, the spatiotemporal assembly point for many r-proteins, including L7, L16 and L17, has recently been deduced by analysing the composition of pre-ribosomal complexes purified from a series of 27S pre-rRNA fragments ([119]). Our data suggest that L14, whose assembly position could unfortunately not be inferred by this latter study, however, seems to assemble slightly later than the L16 r-protein (see below).

Regarding its role in ribosome biogenesis and as expected for an essential 60S r-protein, depletion of L14 leads to a strong shortage of 60S r-subunits. Examination of pre-rRNA processing by pulse-chase, northern blotting and primer extension analyses clearly indicates that this is the consequence of the severe impairment of the conversion of 27S precursors into mature 25S and 5.8S rRNAs. Thus, while levels of $27SA_2$ pre-rRNA do practically not change upon depletion of L14, the $27SA_3$ pre-rRNA mildly accumulates. Levels of the subsequent $27SB_S$ pre-rRNA drastically decreases, but not those of the $27SB_L$ pre-rRNA. In any case, reduced formation of both forms of 7S pre-rRNA and thus of mature 5.8S rRNAs is observed, thus, indicating that upon depletion of L14, maturation of 27SB pre-rRNAs at ITS2 is blocked. As deduced by pulse-chase labelling experiments, 27SB pre-rRNAs are indeed subjected to significant turnover following depletion of L14. These results are compatible with a specific role of L14 in enabling processing of the $27SA_3$ pre-rRNA and its requirement for the efficient maturation of both 27SB pre-rRNA species. Our analyses also show that depletion of L14 causes a mild delay in the pre-rRNA processing events at sites A_0, A_1 and A_2, such that 35S pre-rRNA accumulates and cleavage at the A_3 site precedes those at the earlier sites, leading to reduced formation of 20S pre-rRNA and appearance of some aberrant 23S pre-rRNA. This latter phenotype is observed for almost any mutant that causes a shortage of 60S r-subunits and seems to appear from the sequestration of early *trans*-acting factors on abortive assembly pre-60S intermediates and/or the specific loss of the co-transcriptional cleavage of the nascent pre-rRNA at the A_0–A_2 sites (further discussed in ([81]); see also ([120],[121])). It seems counterintuitive that depletion of L14 could delay the earliest pre-rRNA processing steps and reduce steady-state levels of 20S pre-rRNA without simultaneously affecting $27SA_2$ pre-rRNA levels, unless that the latter could be the result of the stabilization of $27SA_2$ precursor-containing pre-60S intermediates early on during depletion of L14. Moreover, wild-type levels of $27SB_L$ pre-rRNA are still detected in the L14-depleted strain, thus, indicating that in these intermediates, $27SA_2$ pre-rRNA processing could still continue at site B_{1L}

for at least a period of 6 h after depletion of L14. Similar pre-rRNA processing defects have previously been observed upon depletion of other 60S r-proteins and different *trans*-acting factors involved in 60S r-subunit biogenesis. Practically identical defects, including mild accumulation of $27SA_2$, $27SA_3$ and $27SB_L$ pre-rRNAs and depletion of $27SB_S$ and $7S_{S/L}$ pre-rRNAs, have been reported upon mutation in or depletion of L4 (38,122,123), L6 (21), L7 (38,40), L8 (38,40), L16 (38,81,100), L18 (21,38,100), L20 (38,100), L33 (36,38,100) and L36 (101). Similar, but not identical phenotypes have been reported upon mutation in or depletion of L3 (21,35,38), L9 (21), L13 (21), L23 (21), and L32 (38). In the case of L3, no $27SA_3$ and $27SB_S$ pre-rRNAs were detected upon its depletion; thus, L3 has been considered as the earliest acting r-protein in the pre-rRNA processing pathway. In the rest of the cases, both species of 27SB pre-rRNAs were detected, but 7S pre-rRNAs were not produced, indicating that these r-proteins are acting a little bit later in the pre-rRNA processing pathway than L14 or the group of functionally related r-proteins mentioned above. Finally, depletion of a subset of other r-proteins, including L17 (37,114), L19 (38), L25 (uL23) (34,38), L27 (38), L34 (38), L35 (31,37,38) and L37 (37), also lead to impaired cleavage at site C_2 in ITS2. As discussed below, similarly to what we have also observed in the L14-depleted strain, depletion of all above r-proteins leads to intranuclear and/or nucleocytoplasmic transport defects of pre-60S r-particles.

The pre-rRNA processing defects of the L14-depleted strain also closely resemble those described upon loss-of-function mutation in or depletion of distinct 60S r-subunit assembly factors, most of them belonging to the category of the so-called 'A_3 factors'. All these factors are required for $27SA_3$ pre-rRNA processing (revised in (10); see also (81)), and comprise at least the Pwp1 subcomplex (Pwp1, Nop12, Ebp2 and Brx1), the Erb1-Nop7-Ytm1 subcomplex, Nop15, Nsa3/Cic1, Rlp7, Rrp1, and the RNA helicases Drs1 and Has1 (e.g. (87,101,114,116,117,124–136)). From all these factors, depletion of only Ebp2, Pwp1, Erb1, Nop7, Ytm1, Nop15, Nsa3 and Rlp7 has been clearly described to provoke the underaccumulation of $27SB_S$ pre-rRNA without affecting significantly the levels of $27SB_L$ pre-rRNA, which is one of the most remarkable features of the pre-rRNA processing defect of the L14-depleted strain.

Moreover, we have compared the composition of early pre-ribosomal particles purified with the *trans*-acting factor Noc2 before or after depletion of L14. Their pre-rRNA composition indicates that these particles are mostly early to medium intermediates along the maturation pathway of 60S r-subunits. However, the particles purified upon depletion of L14 may correspond to those intermediary precursors that have been able to incorporate all those r-proteins and *trans*-acting factors that are not strictly dependent on the assembly of L14. As depletion of L14 leads to turnover of 27S pre-rRNAs and accumulation of pre-60S r-particles in the nucleus, it is likely that these intermediaries are indeed those particles that we have observed to be retained in the nucle(ol)us, but have not still been targeted for degradation. These particles may arise as the consequence of a structural proofreading checkpoint that impedes the association of different *trans*-acting factors, specially export fac-

tors such as Nmd3, in the disturbed conformational state of 27S pre-rRNA that results in the absence of L14 assembly (see (13,137) for further discussion). The protein composition of these particles indicates that depletion of L14 prevents stable assembly of several r-proteins, among them two distinct groups of proteins can be highlighted: first, the group comprising the r-proteins L17, L39, L26, L37 and L19, all of them surrounding the peptide exit tunnel site, which predominantly bind the domain I of 25S/5.8S rRNAs; second, the group formed by L33, L6 and L20, which all are close neighbors of L14 and bind domain II of 25S rRNA. Remarkably, L16, which directly interacts with L14, L20 and L33 (43), is not significantly affected by the depletion of L14. This result strongly suggests that, despite their physical interaction, the assembly of L14 and L16 is not totally interdependent and that L16 associates earlier than L14 with pre-60S r-particles. The stable association of most *trans*-acting factors belonging to the category known as 'B factors', which are required for cleavage of 27SB pre-rRNAs at site C_2, is negatively affected (10,102). This result is in agreement with the requirement of L14 for 27SB pre-rRNA maturation. Paradoxically, the recruitment of most 'A_3 factors', whose association to pre-60S r-particles is interdependent and are involved in $27SA_3$ pre-rRNA processing (114), remains unaffected or even slightly increases in the purified L14-depleted pre-60S r-particles. This result clearly indicates that, in contrast to other r-proteins such as L8, whose assembly is necessary for the association of the 'A_3 factors' with pre-ribosomal particles (40,100), L14 is not required for the association of these factors with early pre-60S r-particles. Therefore, the $27SA_3$ pre-rRNA processing defect observed upon depletion of L14 is not directly triggered by the failure of 'A_3 factors' to associate with pre-60S r-particles. Instead, the depletion of L14 must rather affect the function of this set of factors during the reorganization of the ITS1/5.8S/ITS2 region of 27S pre-rRNA and the assembly of the r-proteins surrounding the exit tunnel, which have been described to allow efficient 5′-3′ exonucleolytic trimming of $27SA_3$ pre-rRNA to $27SB_S$ pre-rRNA (114). Our results also indicate that the reduced assembly of the r-proteins surrounding the exit tunnel upon depletion of L14 is not the consequence of the absence of 'A_3 factors' from the pre-60S r-particles, but rather the result of the defective formation of their binding sites within the pre-rRNA. Processing of $27SA_2$ pre-rRNA to $27SA_3$ pre-rRNA seems not to be affected upon depletion of L14. Consistently, our results show that L3, which is needed for this step (35), is present in the purified pre-60S r-particles. Moreover, RNase MRP, the endonuclease required for cleavage at site A_3 (for a review, see (138)), must still be efficiently recruited and able to exert its activity upon depletion of L14. It has been reported that *in vitro* cleavage at site A_3 by RNase MRP only required a minimal single-stranded RNA substrate (138–140), thus, this minimal substrate requirements must be present in the L14-depleted pre-60S r-particles.

Globally, our findings are in agreement with those of a previous report on the assembly of r-proteins and association of *trans*-acting factors upon the depletion of r-proteins such as L7, L16, L18, L20, L32 and L33 that bind domain II of 25S/5.8S rRNAs and belong to the neighborhood of L14 (21,100). The comparison of the results of those reports

with the data presented herein strongly suggests that assembly of L14 into early pre-60S r-particles is mutually interdependent with at least that of L6, L20 and L33. L16 seems to assemble earlier than L14 and while its assembly appears to be required for the efficient incorporation of L14, the contrary is not applicable. Consistent with this suggestion, the Granneman lab has recently shown that, among other r-proteins, L16 was roughly/slightly more abundant than L14 in early 90S/66S pre-ribosomal particles purified using the TAP-tagged Rrp5 factor, while both r-proteins were evenly enriched in Nsa2-TAP containing pre-60S particles, which represent later intermediates along the 60S r-subunit maturation pathway [141]. The local alterations that the lack of assembly of any of these proteins must cause in their close environment within domains II and VI (ES39) of 25S rRNA should also negatively affect the assembly of another set of r-proteins, among them L17, L19, L26 and L39 at domain I of 25S/5.8S rRNA. Moreover, these alterations also specifically affect the association of a sub-group of *trans*-acting factors to pre-60S r-particles. Recently, the structures of early yeast pre-60S intermediates have been resolved at high resolution by cryo-EM [51]. These complexes were classified into six distinct states (states A to F), which represent the sequential assembly events along the formation of early nucleolar pre-60S r-particles. The comparison of our iTRAQ data with the r-proteins and *trans*-acting factors that are stably associated with the particles at each state, indicates that the Noc2-TAP containing intermediates accumulating upon depletion of L14 belong to the state A of 60S r-subunit maturation; these intermediates lacks the terminal structural domain formed by L14 and its neighboring L6, L16, L20 and L33 r-proteins ('L14 domain') but contain both the r-proteins and the set of *trans*-acting factors, most of them belonging to the A$_3$ cluster, that stably associate with the other two structurally independent domains ('Central domain' and 'Foot domain') of these particles (see Supplementary Figure S15 and Supplementary Tables S4 and S5). This comparison also shows that all *trans*-acting factors, most of them belonging to the B cluster, that are co-depleted with L14, except the RNA helicases Dbp10 and Spb4, belong to the state E pre-60S category; state E particles also contain most r-proteins, including those surrounding the peptide exit tunnel, that are co-depleted with L14 but are not part of its neighborhood (Supplementary Figures S16 and S17; Supplementary Tables S5 and S6). The non-identification of Dbp10 and Spb4 within state E pre-60S r-particles likely reflects the labile/transient interactions of these enzymes with the pre-ribosomal particles and, thus, their loss during purification. Taken together, these results strongly suggest that progression of pre-60S r-particles from early state A to later state E is impaired upon depletion of L14, therefore, revealing the series of dissociation/association events that physiologically occur during the transition from one state to the next, more mature one. Finally, the fact that the depletion of a group of interdependent r-proteins leads to similar changes in the composition of early pre-60S r-particles explains in a logical and simple manner why the pre-rRNA processing phenotypes detected upon the depletion of all these r-proteins by different authors are practically identical.

We have also studied the functional relationship between the eukaryote-specific C-terminal tails of L14 and L16, which are packed against each other in the mature 60S r-subunit [41,43]. Remarkably, the cryo-EM structure of early state A pre-60S r-particles [51] undoubtedly reveals that the environment formed by the r-proteins L14 and L16 and the rRNA expansion segments ES7^L and ES39^L, which sandwich the C-terminal tails of these r-proteins, adopts its final (mature) conformation very early during the 60S r-subunit assembly process (Supplementary Figure S18). It has been previously shown that the truncation of the last 16 amino acids of L14A (*rpl14A-N122* allele), when expressed as the sole source of L14 from a centromeric plasmid, confers a mild 60S r-biogenesis defect that slightly compromises growth at 30°C [71]. Here, we show that longer truncations are lethal. Similarly, deletion of the last 18 amino acids of L16B (*rpl16B-N180* allele) does not cause any deleterious effect; however, truncation of 28 or more amino acids of the C-terminal extension of L16B does not support growth [81,100]. Moreover, our study revealed a specific genetic interaction between the viable *rpl14A-N122* and *rpl16B-N180* alleles and mutants of genes encoding 60S r-subunit assembly factors belonging to the so-called Mak5 cluster. These results suggest that the putative RNA helicase Mak5 and its genetically interacting partners Ebp2 and Nop16 could facilitate the stable assembly of these two r-proteins into early pre-60S r-particles, with the C-terminal extensions of the two r-proteins and perhaps those of Mak5 and Ebp2 possibly playing a relevant role. We have also co-expressed the L14A-N122 and the L16B-N180 variant r-proteins as the sole cellular source of L14 and L16, respectively, in yeast cells that are wild type for the Mak5 cluster factors. Our results indicate that this combination, although it does not lead to any synergistic defect under normal growth conditions (i.e. YPD medium, 30°C), is unable to support growth on media containing a sub-lethal concentration of paromomycin. This result suggests that the complete interaction of the C-terminal ends of L14 and L16 is not strictly required for 60S r-subunit assembly, but it is at least critical for some, yet to be unveiled, functional aspects of 60S r-subunits.

In summary, our study has revealed that assembly of L14 into early pre-60S r-particles is required for the progression of 27SA pre-rRNA processing. Defects in these steps are likely the consequence of significant changes in the structure of the pre-60S r-particles, arising from the failure of assembly of a set of mutually interdependent r-proteins, which in turn are necessary for the association of a set of B *trans*-acting factors. This scenario matches perfectly well with the first steps during the maturation of stable early pre-60S r-particles whose structures have recently been solved by cryo-EM [51]. Further studies are required to obtain a molecular understanding of the connection between the assembly of the L14-interdependent r-proteins and the activation of the 'A$_3$ factors' as well as the association of the 'B factors'. Finally, it has been shown that some neighboring r-proteins such as L5 and L11 [56] or S14 (uS11) and S26 (eS26) [142] are preferentially delivered to pre-ribosomal particles as sub-complexes associated with dedicated *trans*-acting factors. Whether this is also the case for L14 and any

of its close r-protein partners is an interesting issue that is worth to being explored by future studies.

SUPPLEMENTARY DATA

Supplementary Data are available at NAR Online.

ACKNOWLEDGEMENTS

FUNDING

REFERENCES

1. Wilson,D.N. and Doudna Cate,J.H. (2012) The structure and function of the eukaryotic ribosome. *Cold Spring Harb. Perspect. Biol.*, **4**, a011536.
2. Melnikov,S., Ben-Shem,A., Garreau de Loubresse,N., Jenner,L., Yusupova,G. and Yusupov,M. (2012) One core, two shells: bacterial and eukaryotic ribosomes. *Nat. Struct. Mol. Biol.*, **19**, 560–567.
3. Fernández-Pevida,A., Martín-Villanueva,S., Murat,G., Lacombe,T., Kressler,D. and de la Cruz,J. (2016) The eukaryote-specific N-terminal extension of ribosomal protein S31 contributes to the assembly and function of 40S ribosomal subunits. *Nucleic Acids Res.*, **44**, 7777–7791.
4. Mauro,V.P. and Edelman,G.M. (2002) The ribosome filter hypothesis. *Proc. Natl. Acad. Sci. U.S.A.*, **99**, 12031–12036.
5. Sauert,M., Temmel,H. and Moll,I. (2015) Heterogeneity of the translational machinery: variations on a common theme. *Biochimie*, **114**, 39–47.
6. Xue,S. and Barna,M. (2012) Specialized ribosomes: a new frontier in gene regulation and organismal biology. *Nat. Rev. Mol. Cell. Biol.*, **13**, 355–369.
7. Armache,J.P., Anger,A.M., Marquez,V., Franckenberg,S., Frohlich,T., Villa,E., Berninghausen,O., Thomm,M., Arnold,G.J., Beckmann,R. *et al.* (2013) Promiscuous behaviour of archaeal ribosomal proteins: implications for eukaryotic ribosome evolution. *Nucleic Acids Res.*, **41**, 1284–1293.
8. Shajani,Z., Sykes,M.T. and Williamson,J.R. (2011) Assembly of bacterial ribosomes. *Annu. Rev. Biochem.*, **80**, 501–526.
9. de la Cruz,J., Karbstein,K. and Woolford,J.L. Jr. (2015) Functions of ribosomal proteins in assembly of eukaryotic ribosomes in vivo. *Annu. Rev. Biochem.*, **84**, 93–129.
10. Woolford,J.L. Jr. and Baserga,S.J. (2013) Ribosome biogenesis in the yeast *Saccharomyces cerevisiae*. *Genetics*, **195**, 643–681.
11. Gerhardy,S., Menet,A.M., Pena,C., Petkowski,J.J. and Panse,V.G. (2014) Assembly and nuclear export of pre-ribosomal particles in budding yeast. *Chromosoma*, **123**, 327–344.
12. Udem,S.A. and Warner,J.R. (1973) The cytoplasmic maturation of a ribosomal precursor ribonucleic acid in yeast. *J. Biol. Chem.*, **248**, 1412–1416.
13. Panse,V.G. and Johnson,A.W. (2010) Maturation of eukaryotic ribosomes: acquisition of functionality. *Trends Biochem. Sci.*, **35**, 260–266.
14. Trapman,J., Retèl,J. and Planta,R.J. (1975) Ribosomal precursor particles from yeast. *Exp. Cell Res.*, **90**, 95–104.
15. Kressler,D., Hurt,E. and Bassler,J. (2010) Driving ribosome assembly. *Biochim. Biophys. Acta*, **1803**, 673–683.
16. Karbstein,K. (2013) Quality control mechanisms during ribosome maturation. *Trends Cell Biol.*, **23**, 242–250.
17. Ferreira-Cerca,S., Pöll,G., Kuhn,H., Neueder,A., Jakob,S., Tschochner,H. and Milkereit,P. (2007) Analysis of the *in vivo* assembly pathway of eukaryotic 40S ribosomal proteins. *Mol. Cell*, **28**, 446–457.
18. Hector,R.D., Burlacu,E., Aitken,S., Bihan,T.L., Tuijtel,M., Zaplatina,A., Cook,A.G. and Granneman,S. (2014) Snapshots of pre-rRNA structural flexibility reveal eukaryotic 40S assembly dynamics at nucleotide resolution. *Nucleic Acids Res.*, **42**, 12138–12154.
19. Ohmayer,U., Gamalinda,M., Sauert,M., Ossowski,J., Poll,G., Linnemann,J., Hierlmeier,T., Pérez-Fernández,J., Kumcuoglu,B., Léger-Silvestre,I. *et al.* (2013) Studies on the assembly characteristics of large subunit ribosomal proteins in *S. cerevisae*. *PLoS One*, **8**, e68412.
20. Davis,J.H., Tan,Y.Z., Carragher,B., Potter,C.S., Lyumkis,D. and Williamson,J.R. (2016) Modular assembly of the bacterial large ribosomal subunit. *Cell*, **167**, 1610–1622.
21. Gamalinda,M., Ohmayer,U., Jakovljevic,J., Kumcuoglu,B., Woolford,J., Mbom,B., Lin,L. and Woolford,J.L. Jr. (2014) A hierarchical model for assembly of eukaryotic 60S ribosomal subunit domains. *Genes Dev.*, **28**, 198–210.
22. Kruiswijk,T., Planta,R.J. and Krop,J.M. (1978) The course of the assembly of ribosomal subunits in yeast. *Biochim. Biophys. Acta*, **517**, 378–389.
23. Warner,J.R. (1971) The assembly of ribosomes in yeast. *J. Biol. Chem.*, **246**, 447–454.
24. Harnpicharnchai,P., Jakovljevic,J., Horsey,E., Miles,T., Roman,J., Rout,M., Meagher,D., Imai,B., Guo,Y., Brame,C.J. *et al.* (2001) Composition and functional characterization of yeast 66S ribosome assembly intermediates. *Mol. Cell*, **8**, 505–515.
25. Bassler,J., Grandi,P., Gadal,O., Lessmann,T., Petfalski,E., Tollervey,D., Lechner,J. and Hurt,E. (2001) Identification of a 60S preribosomal particle that is closely linked to nuclear export. *Mol. Cell*, **8**, 517–529.
26. Grandi,P., Rybin,V., Bassler,J., Petfalski,E., Strauss,D., Marzioch,M., Schäfer,T., Kuster,B., Tschochner,H., Tollervey,D. *et al.* (2002) 90S pre-ribosomes include the 35S pre-rRNA, the U3 snoRNP, and 40S subunit processing factors but predominantly lack 60S synthesis factors. *Mol. Cell*, **10**, 105–115.
27. Schäfer,T., Strauss,D., Petfalski,E., Tollervey,D. and Hurt,E. (2003) The path from nucleolar 90S to cytoplasmic 40S pre-ribosomes. *EMBO J.*, **22**, 1370–1380.
28. Gavin,A.C., Bosche,M., Krause,R., Grandi,P., Marzioch,M., Bauer,A., Schultz,J., Rick,J.M., Michon,A.M., Cruciat,C.M. *et al.* (2002) Functional organization of the yeast proteome by systematic analysis of protein complexes. *Nature*, **415**, 141–147.
29. Krogan,N.J., Cagney,G., Yu,H., Zhong,G., Guo,X., Ignatchenko,A., Li,J., Pu,S., Datta,N., Tikuisis,A.P. *et al.* (2006) Global landscape of protein complexes in the yeast *Saccharomyces cerevisiae*. *Nature*, **440**, 637–643.
30. Altvater,M., Chang,Y., Melnik,A., Occhipinti,L., Schütz,S., Rothenbusch,U., Picotti,P. and Panse,V.G. (2012) Targeted proteomics reveals compositional dynamics of 60S pre-ribosomes after nuclear export. *Mol. Syst. Biol.*, **8**, 628.
31. Babiano,R. and de la Cruz,J. (2010) Ribosomal protein L35 is required for 27SB pre-rRNA processing in *Saccharomyces cerevisiae*. *Nucleic Acids Res.*, **38**, 5177–5192.
32. Rodríguez-Mateos,M., García-Gómez,J.J., Francisco-Velilla,R., Remacha,M., de la Cruz,J. and Ballesta,J.P.G. (2009) Role and dynamics of the ribosomal protein P0 and its related *trans*-acting factor Mrt4 during ribosome assembly in *Saccharomyces cerevisiae*. *Nucleic Acids Res.*, **37**, 7519–7532.

33. Fernández-Pevida,A., Rodríguez-Galán,O., Díaz-Quintana,A., Kressler,D. and Cruz,J. (2012) Yeast ribosomal protein L40 assembles late into precursor 60S ribosomes and is required for their cytoplasmic maturation. *J. Biol. Chem.*, **287**, 38390–38407.

34. van Beekvelt,C.A., de Graaff-Vincent,M., Faber,A.W., van't Riet,J., Venema,J. and Raué,H.A. (2001) All three functional domains of the large ribosomal subunit protein L25 are required for both early and late pre-rRNA processing steps in *Saccharomyces cerevisiae*. *Nucleic Acids Res.*, **29**, 5001–5008.

35. Rosado,I.V., Kressler,D. and de la Cruz,J. (2007) Functional analysis of *Saccharomyces cerevisiae* ribosomal protein Rpl3p in ribosome synthesis. *Nucleic Acids Res.*, **35**, 4203–4213.

36. Martín-Marcos,P., Hinnebusch,A.G. and Tamame,M. (2007) Ribosomal protein L33 is required for ribosome biogenesis, subunit joining, and repression of *GCN4* translation. *Mol. Cell. Biol.*, **27**, 5968–5985.

37. Gamalinda,M., Jakovljevic,J., Babiano,R., Talkish,J., de la Cruz,J. and Woolford,J.L. Jr. (2013) Yeast polypeptide exit tunnel ribosomal proteins L17, L35 and L37 are necessary to recruit late-assembling factors required for 27SB pre-rRNA processing. *Nucleic Acids Res.*, **41**, 1965–1983.

38. Pöll,G., Braun,T., Jakovljevic,J., Neueder,A., Jakob,S., Woolford,J.L. Jr., Tschochner,H. and Milkereit,P. (2009) rRNA maturation in yeast cells depleted of large ribosomal subunit proteins. *PLoS One*, **4**, e8249.

39. Ferreira-Cerca,S., Pöll,G., Gleizes,P.E., Tschochner,H. and Milkereit,P. (2005) Roles of eukaryotic ribosomal proteins in maturation and transport of pre-18S rRNA and ribosome function. *Mol. Cell*, **20**, 263–275.

40. Jakovljevic,J., Ohmayer,U., Gamalinda,M., Talkish,J., Alexander,L., Linnemann,J., Milkereit,P. and Woolford,J.L. Jr. (2012) Ribosomal proteins L7 and L8 function in concert with six A_3 assembly factors to propagate assembly of domains I and II of 25S rRNA in yeast 60S ribosomal subunits. *RNA*, **18**, 1805–1822.

41. Klinge,S., Voigts-Hoffmann,F., Leibundgut,M., Arpagaus,S. and Ban,N. (2011) Crystal structure of the eukaryotic 60S ribosomal subunit in complex with initiation factor 6. *Science*, **334**, 941–948.

42. Rabl,J., Leibundgut,M., Ataide,S.F., Haag,A. and Ban,N. (2011) Crystal structure of the eukaryotic 40S ribosomal subunit in complex with initiation factor 1. *Science*, **331**, 730–736.

43. Ben-Shem,A., Garreau de Loubresse,N., Melnikov,S., Jenner,L., Yusupova,G. and Yusupov,M. (2011) The structure of the eukaryotic ribosome at 3.0 Å resolution. *Science*, **334**, 1524–1529.

44. Wu,S., Tutuncuoglu,B., Yan,K., Brown,H., Zhang,Y., Tan,D., Gamalinda,M., Yuan,Y., Li,Z., Jakovljevic,J. *et al.* (2016) Diverse roles of assembly factors revealed by structures of late nuclear pre-60S ribosomes. *Nature*, **534**, 133–137.

45. Leidig,C., Thoms,M., Holdermann,I., Bradatsch,B., Berninghausen,O., Bange,G., Sinning,I., Hurt,E. and Beckmann,R. (2014) 60S ribosome biogenesis requires rotation of the 5S ribonucleoprotein particle. *Nat. Commun.*, **5**, 3491.

46. Greber,B.J., Gerhardy,S., Leitner,A., Leibundgut,M., Salem,M., Boehringer,D., Leulliot,N., Aebersold,R., Panse,V.G. and Ban,N. (2016) Insertion of the biogenesis factor Rei1 probes the ribosomal tunnel during 60S maturation. *Cell*, **164**, 91–102.

47. Weis,F., Giudice,E., Churcher,M., Jin,L., Hilcenko,C., Wong,C.C., Traynor,D., Kay,R.R. and Warren,A.J. (2015) Mechanism of eIF6 release from the nascent 60S ribosomal subunit. *Nat. Struct. Mol. Biol.*, **22**, 914–919.

48. Ma,C., Wu,S., Li,N., Chen,Y., Yan,K., Li,Z., Zheng,L., Lei,J., Woolford,J.L. Jr. and Gao,N. (2017) Structural snapshot of cytoplasmic pre-60S ribosomal particles bound by Nmd3, Lsg1, Tif6 and Reh1. *Nat. Struct. Mol. Biol.*, **24**, 214–220.

49. Johnson,M.C., Ghalei,H., Doxtader,K.A., Karbstein,K. and Stroupe,M.E. (2017) Structural heterogeneity in pre-40S ribosomes. *Structure*, **25**, 329–340.

50. Strunk,B.S., Loucks,C.R., Su,M., Vashisth,H., Cheng,S., Schilling,J., Brooks,C.L. III, Karbstein,K. and Skiniotis,G. (2011) Ribosome assembly factors prevent premature translation initiation by 40S assembly intermediates. *Science*, **333**, 1449–1453.

51. Kater,L., Thoms,M., Barrio-García,C., Cheng,J., Ismail,S., Ahmed,Y.L., Bange,G., Kressler,D., Berninghausen,O., Sinning,I. *et al.* (2017) Visualizing the assembly pathway of nucleolar pre-60S ribosomes. *Cell*, **171**, 1599–1610.

52. Greber,B.J. (2016) Mechanistic insight into eukaryotic 60S ribosomal subunit biogenesis by cryo-electron microscopy. *RNA*, **22**, 1643–1662.

53. Biedka,S., Wu,S., LaPeruta,A.J., Gao,N. and Woolford,J.L. Jr. (2017) Insights into remodeling events during eukaryotic large ribosomal subunit assembly provided by high resolution cryo-EM structures. *RNA Biol.*, **14**, 1306–1313.

54. Kressler,D., Hurt,E. and Bassler,J. (2017) A puzzle of life: rafting ribosomal subunits. *Trends Biochem. Sci.*, **42**, 640–654.

55. Mitterer,V., Murat,G., Rety,S., Blaud,M., Delbos,L., Stanborough,T., Bergler,H., Leulliot,N., Kressler,D. and Pertschy,B. (2016) Sequential domain assembly of ribosomal protein S3 drives 40S subunit maturation. *Nat. Commun.*, **7**, 10336.

56. Kressler,D., Bange,G., Ogawa,Y., Stjepanovic,G., Bradatsch,B., Pratte,D., Amlacher,S., Strauss,D., Yoneda,Y., Katahira,J. *et al.* (2012) Synchronizing nuclear import of ribosomal proteins with ribosome assembly. *Science*, **338**, 666–671.

57. Huber,F.M. and Hoelz,A. (2017) Molecular basis for protection of ribosomal protein L4 from cellular degradation. *Nat. Commun.*, **8**, 14354.

58. Madru,C., Lebaron,S., Blaud,M., Delbos,L., Pipoli,J., Pasmant,E., Réty,S. and Leulliot,N. (2015) Chaperoning 5S RNA assembly. *Genes Dev.*, **29**, 1432–1446.

59. Zhang,J., Harnpicharnchai,P., Jakovljevic,J., Tang,L., Guo,Y., Oeffinger,M., Rout,M.P., Hiley,S.L., Hughes,T. and Woolford,J.L. Jr. (2007) Assembly factors Rpf2 and Rrs1 recruit 5S rRNA and ribosomal proteins rpL5 and rpL11 into nascent ribosomes. *Genes Dev.*, **21**, 2580–2592.

60. O'Donohue,M.F., Choesmel,V., Faubladier,M., Fichant,G. and Gleizes,P.E. (2010) Functional dichotomy of ribosomal proteins during the synthesis of mammalian 40S ribosomal subunits. *J. Cell Biol.*, **190**, 853–866.

61. Mizushima,S. and Nomura,M. (1970) Assembly mapping of 30S ribosomal proteins in *E. coli*. *Nature*, **226**, 1214–1218.

62. Chaker-Margot,M., Hunziker,M., Barandun,J., Dill,B.D. and Klinge,S. (2015) Stage-specific assembly events of the 6-MDa small-subunit processome initiate eukaryotic ribosome biogenesis. *Nat. Struct. Mol. Biol.*, **22**, 920–923.

63. Zhang,L., Wu,C., Cai,G., Chen,S. and Ye,K. (2016) Stepwise and dynamic assembly of the earliest precursors of small ribosomal subunits in yeast. *Genes Dev.*, **30**, 718–732.

64. Chaker-Margot,M., Barandun,J., Hunziker,M. and Klinge,S. (2016) Architecture of the yeast small subunit processome. *Science*, **355**, eaal1880.

65. Kornprobst,M., Turk,M., Kellner,N., Cheng,J., Flemming,D., Kos-Braun,I., Kos,M., Thoms,M., Berninghausen,O., Beckmann,R. *et al.* (2016) Architecture of the 90S pre-ribosome: a structural view on the birth of the eukaryotic ribosome. *Cell*, **166**, 380–393.

66. Sun,Q., Zhu,X., Qi,J., An,W., Lan,P., Tan,D., Chen,R., Wang,B., Zheng,S., Zhang,C. *et al.* (2017) Molecular architecture of the 90S small subunit pre-ribosome. *eLife*, **6**, e22086.

67. Ban,N., Beckmann,R., Cate,J.H., Dinman,J.D., Dragon,F., Ellis,S.R., Lafontaine,D.L., Lindahl,L., Liljas,A., Lipton,J.M. *et al.* (2014) A new system for naming ribosomal proteins. *Curr. Opin. Struct. Biol.*, **24**, 165–169.

68. Konikkat,S. and Woolford,J.L. Jr. (2016) Principles of 60S ribosomal subunit assembly emerging from recent studies in yeast. *Biochem J.*, **474**, 195–214.

69. Nicolas,E., Parisot,P., Pinto-Monteiro,C., de Walque,R., De Vleeschouwer,C. and Lafontaine,D.L. (2016) Involvement of human ribosomal proteins in nucleolar structure and p53-dependent nucleolar stress. *Nat Commun.*, **7**, 11390.

70. Nakao,A., Yoshihama,M. and Kenmochi,N. (2004) RPG: the ribosomal protein gene database. *Nucleic Acids Res.*, **32**, D168–D170.

71. Pratte,D., Singh,U., Murat,G. and Kressler,D. (2013) Mak5 and Ebp2 act together on early pre-60S particles and their reduced functionality bypasses the requirement for the essential pre-60S factor Nsa1. *PLoS One*, **8**, e82741.

72. Robledo,S., Idol,R.A., Crimmins,D.L., Ladenson,J.H., Mason,P.J. and Bessler,M. (2008) The role of human ribosomal proteins in the maturation of rRNA and ribosome production. *RNA*, **14**, 1918–1929.

73. Longtine,M.S., McKenzie,A. III, Demarini,D.J., Shah,N.G., Wach,A., Brachat,A., Philippsen,P. and Pringle,J.R. (1998) Additional modules for versatile and economical PCR-based gene deletion and modification in *Saccharomyces cerevisiae*. *Yeast*, **14**, 953–961.

74. Babiano,R., Gamalinda,M., Woolford,J.L. Jr. and de la Cruz,J. (2012) *Saccharomyces cerevisiae* ribosomal protein L26 is not essential for ribosome assembly and function. *Mol. Cell. Biol.*, **32**, 3228–3241.

75. Gietz,D., St. Jean,A., Woods,R.A. and Schiestl,R.H. (1992) Improved method for high efficiency transformation of intact yeast cells. *Nucleic Acids Res.*, **20**, 1425.

76. Kressler,D., de la Cruz,J., Rojo,M. and Linder,P. (1997) Fal1p is an essential DEAD-box protein involved in 40S-ribosomal-subunit biogenesis in *Saccharomyces cerevisiae*. *Mol. Cell. Biol.*, **17**, 7283–7294.

77. Kressler,D., de la Cruz,J., Rojo,M. and Linder,P. (1998) Dbp6p is an essential putative ATP-dependent RNA helicase required for 60S-ribosomal-subunit assembly in *Saccharomyces cerevisiae*. *Mol. Cell. Biol.*, **18**, 1855–1865.

78. Ausubel,F.M., Brent,R., Kingston,R.E., Moore,D.D., Seidman,J.G., Smith,J.A. and Struhl,K. (1994) *Current Protocols in Molecular Biology*. John Wiley & Sons, Inc., NY, pp. 13.10.11–13.14.17.

79. Venema,J., Planta,R.J. and Raué,H.A. (1998) In: Martin,R (ed). *Protein Synthesis: Methods and Protocols*. Humana Press, Totowa, pp. 257–270.

80. García-Gómez,J.J., Lebaron,S., Froment,C., Monsarrat,B., Henry,Y. and de la Cruz,J. (2011) Dynamics of the putative RNA helicase Spb4 during ribosome assembly in *Saccharomyces cerevisiae*. *Mol. Cell. Biol.*, **31**, 4156–4164.

81. Espinar-Marchena,F.J., Fernández-Fernández,J., Rodríguez-Galán,O., Fernández-Pevida,A., Babiano,R. and de la Cruz,J. (2016) Role of the yeast ribosomal protein L16 in ribosome biogenesis. *FEBS J.*, **283**, 2968–2985.

82. Petitjean,A., Bonneaud,N. and Lacroute,F. (1995) The duplicated *Saccharomyces cerevisiae* gene *SSM1* encodes a eucaryotic homolog of the eubacterial and archaebacterial L1 ribosomal protein. *Mol. Cell. Biol.*, **15**, 5071–5081.

83. Dieci,G., Bottarelli,L. and Ottonello,S. (2005) A general procedure for the production of antibody reagents against eukaryotic ribosomal proteins. *Protein Pept. Lett.*, **12**, 555–560.

84. Tron,T., Yang,M., Dick,F.A., Schmitt,M.E. and Trumpower,B.L. (1995) QSR1, an essential yeast gene with a genetic relationship to a subunit of the mitochondrial cytochrome bc₁ complex, is homologous to a gene implicated in eukaryotic cell differentiation. *J. Biol. Chem.*, **270**, 9961–9970.

85. Gautschi,M., Lilie,H., Funfschilling,U., Mun,A., Ross,S., Lithgow,T., Rucknagel,P. and Rospert,S. (2001) RAC, a stable ribosome-associated complex in yeast formed by the DnaK-DnaJ homologs Ssz1p and zuotin. *Proc. Natl. Acad. Sci. U.S.A.*, **98**, 3762–3767.

86. Wegrecki,M., Rodriguez-Galán,O., de la Cruz,J. and Bravo,J. (2015) The structure of Erb1-Ytm1 complex reveals the functional importance of a high-affinity binding between two beta-propellers during the assembly of large ribosomal subunits in eukaryotes. *Nucleic Acids Res.*, **43**, 11017–11030.

87. Emery,B., de la Cruz,J., Rocak,S., Deloche,O. and Linder,P. (2004) Has1p, a member of the DEAD-box family, is required for 40S ribosomal subunit biogenesis in *Saccharomyces cerevisiae*. *Mol. Microbiol.*, **52**, 141–158.

88. Rodríguez-Mateos,M., Abia,D., García-Gómez,J.J., Morreale,A., de la Cruz,J., Santos,C., Remacha,M. and Ballesta,J.P.G. (2009) The amino terminal domain from Mrt4 protein can functionally replace the RNA binding domain of the ribosomal P0 protein. *Nucleic Acids Res.*, **37**, 3514–3521.

89. Jakob,S., Ohmayer,U., Neueder,A., Hierlmeier,T., Perez-Fernandez,J., Hochmuth,E., Deutzmann,R., Griesenbeck,J., Tschochner,H. and Milkereit,P. (2012) Interrelationships between yeast ribosomal protein assembly events and transient ribosome biogenesis factors interactions in early pre-ribosomes. *PLoS One*, **7**, e32552.

90. Kosugi,S., Hasebe,M., Tomita,M. and Yanagawa,H. (2009) Systematic identification of cell cycle-dependent yeast nucleocytoplasmic shuttling proteins by prediction of composite motifs. *Proc. Natl. Acad. Sci. U.S.A.*, **106**, 10171–10176.

91. Brameier,M., Krings,A. and MacCallum,R.M. (2007) NucPred–predicting nuclear localization of proteins. *Bioinformatics*, **23**, 1159–1160.

92. Ho,J.H.-N., Kallstrom,G. and Johnson,A.W. (2000) Nmd3p is a Crm1p-dependent adapter protein for nuclear export of the large ribosomal subunit. *J. Cell Biol.*, **151**, 1057–1066.

93. West,M., Hedges,J.B., Chen,A. and Johnson,A.W. (2005) Defining the order in which Nmd3p and Rpl10p load onto nascent 60S ribosomal subunits. *Mol. Cell. Biol.*, **25**, 3802–3813.

94. Steffen,K.K., McCormick,M.A., Pham,K.M., Mackay,V.L., Delaney,J.R., Murakami,C.J., Kaeberlein,M. and Kennedy,B.K. (2012) Ribosome deficiency protects against ER stress in *Saccharomyces cerevisiae*. *Genetics*, **191**, 107–118.

95. Zaman,S., Lippman,S.I., Zhao,X. and Broach,J.R. (2008) How *Saccharomyces* responds to nutrients. *Annu. Rev. Genet.*, **42**, 27–81.

96. de la Cruz,J., Sanz-Martinez,E. and Remacha,M. (2005) The essential WD-repeat protein Rsa4p is required for rRNA processing and intra-nuclear transport of 60S ribosomal subunits. *Nucleic Acids Res.*, **33**, 5728–5739.

97. Hurt,E., Hannus,S., Schmelzl,B., Lau,D., Tollervey,D. and Simos,G. (1999) A novel *in vivo* assay reveals inhibition of ribosomal nuclear export in Ran-cycle and nucleoporin mutants. *J. Cell Biol.*, **144**, 389–401.

98. Milkereit,P., Gadal,O., Podtelejnikov,A., Trumtel,S., Gas,N., Petfalski,E., Tollervey,D., Mann,M., Hurt,E. and Tschochner,H. (2001) Maturation and intranuclear transport of pre-ribosomes requires Noc proteins. *Cell*, **105**, 499–509.

99. Hierlmeier,T., Merl,J., Sauert,M., Perez-Fernandez,J., Schultz,P., Bruckmann,A., Hamperl,S., Ohmayer,U., Rachel,R., Jacob,A. *et al.* (2012) Rrp5p, Noc1p and Noc2p form a protein module which is part of early large ribosomal subunit precursors in S. cerevisiae. *Nucleic Acids Res.*, **41**, 1191–1210.

100. Ohmayer,U., Gil-Hernández,Á., Sauert,M., Martín-Marcos,P., Tamame,M., Tschochner,H., Griesenbeck,J. and Milkereit,P. (2015) Studies on the coordination of ribosomal protein assembly events involved in processing and stabilization of yeast early large ribosomal subunit precursors. *PLoS One*, **10**, e0143768.

101. Wan,K., Yabuki,Y. and Mizuta,K. (2014) Roles of Ebp2 and ribosomal protein L36 in ribosome biogenesis in *Saccharomyces cerevisiae*. *Curr. Genet.*, **61**, 31–41.

102. Talkish,J., Zhang,J., Jakovljevic,J., Horsey,E.W. and Woolford,J.L. Jr. (2012) Hierarchical recruitment into nascent ribosomes of assembly factors required for 27SB pre-rRNA processing in *Saccharomyces cerevisiae*. *Nucleic Acids Res.*, **40**, 8646–8661.

103. Kressler,D., Rojo,M., Linder,P. and de la Cruz,J. (1999) Spb1p is a putative methyltransferase required for 60S ribosomal subunit biogenesis in *Saccharomyces cerevisiae*. *Nucleic Acids Res.*, **27**, 4598–4608.

104. Lebreton,A., Saveanu,C., Decourty,L., Jacquier,A. and Fromont-Racine,M. (2006) Nsa2 is an unstable, conserved factor required for the maturation of 27SB pre-rRNAs. *J. Biol. Chem.*, **281**, 27099–27108.

105. Burger,F., Daugeron,M.-C. and Linder,P. (2000) Dbp10p, a putative RNA helicase from *Saccharomyces cerevisiae* required for ribosome biogenesis. *Nucleic Acids Res.*, **28**, 2315–2323.

106. Saveanu,C., Namane,A., Gleizes,P.E., Lebreton,A., Rousselle,J.C., Noaillac-Depeyre,J., Gas,N., Jacquier,A. and Fromont-Racine,M. (2003) Sequential protein association with nascent 60S ribosomal particles. *Mol. Cell. Biol.*, **23**, 4449–4460.

107. Hong,B., Brockenbrough,J.S., Wu,P. and Aris,J.P. (1997) Nop2p is required for pre-rRNA processing and 60S ribosome subunit synthesis in yeast. *Mol. Cell. Biol.*, **17**, 378–388.

108. Zanchin,N.I.T., Roberts,P., DeSilva,A., Sherman,F. and Goldfarb,D.S. (1997) *Saccharomyces cerevisiae* Nip7p is required for efficient 60S ribosome subunit biogenesis. *Mol. Cell. Biol.*, **17**, 5001–5015.

109. Basu,U., Si,K., Warner,J.R. and Maitra,U. (2001) The *Saccharomyces cerevisiae* TIF6 gene encoding translation initiation factor 6 is required for 60S ribosomal subunit biogenesis. *Mol. Cell. Biol.*, **75**, 1453–1462.

110. de la Cruz,J., Kressler,D., Rojo,M., Tollervey,D. and Linder,P. (1998) Spb4p, an essential putative RNA helicase, is required for a

late step in the assembly of 60S ribosomal subunits in *Saccharomyces cerevisiae. RNA*, **4**, 1268–1281.

111. Manikas,R.G., Thomson,E., Thoms,M. and Hurt,E. (2016) The K+-dependent GTPase Nug1 is implicated in the association of the helicase Dbp10 to the immature peptidyl transferase centre during ribosome maturation. *Nucleic Acids Res.*, **44**, 1800–1812.

112. Bassler,J., Kallas,M. and Hurt,E. (2006) The NUG1 GTPase reveals and N-terminal RNA-binding domain that is essential for association with 60 S pre-ribosomal particles. *J. Biol. Chem.*, **281**, 24737–24744.

113. Yamada,H., Horigome,C., Okada,T., Shirai,C. and Mizuta,K. (2007) Yeast Rrp14p is a nucleolar protein involved in both ribosome biogenesis and cell polarity. *RNA*, **13**, 1977–1987.

114. Sahasranaman,A., Dembowski,J., Strahler,J., Andrews,P., Maddock,J. and Woolford,J.L. Jr. (2011) Assembly of *Saccharomyces cerevisiae* 60S ribosomal subunits: role of factors required for 27S pre-rRNA processing. *EMBO J.*, **30**, 4020–4032.

115. Miles,T.D., Jakovljevic,J., Horsey,E.W., Harnpicharnchai,P., Tang,L. and Woolford,J.L. Jr. (2005) Ytm1, Nop7, and Erb1 form a complex necessary for maturation of yeast 66S preribosomes. *Mol. Cell. Biol.*, **25**, 10419–10432.

116. Merl,J., Jakob,S., Ridinger,K., Hierlmeier,T., Deutzmann,R., Milkereit,P. and Tschochner,H. (2010) Analysis of ribosome biogenesis factor-modules in yeast cells depleted from pre-ribosomes. *Nucleic Acids Res.*, **38**, 3068–3080.

117. Dembowski,J.A., Kuo,B. and Woolford,J.L. Jr. (2013) Has1 regulates consecutive maturation and processing steps for assembly of 60S ribosomal subunits. *Nucleic Acids Res.*, **41**, 7889–7904.

118. Babiano,R., Badis,G., Saveanu,C., Namane,A., Doyen,A., Díaz-Quintana,A., Jacquier,A., Fromont-Racine,M. and de la Cruz,J. (2013) Yeast ribosomal protein L7 and its homologue Rlp7 are simultaneously present at distinct sites on pre-60S ribosomal particles. *Nucleic Acids Res.*, **41**, 9461–9470.

119. Chen,W., Xie,Z., Yang,F. and Ye,K. (2017) Stepwise assembly of the earliest precursors of large ribosomal subunits in yeast. *Nucleic Acids Res.*, **45**, 6837–6847.

120. Axt,K., French,S.L., Beyer,A.L. and Tollervey,D. (2014) Kinetic analysis demonstrates a requirement for the Rat1 exonuclease in cotranscriptional pre-rRNA cleavage. *PLoS One*, **9**, e85703.

121. Talkish,J., Biedka,S., Jakovljevic,J., Zhang,J., Tang,L., Strahler,J.R., Andrews,P.C., Maddock,J.R. and Woolford,J.L. Jr. (2016) Disruption of ribosome assembly in yeast blocks cotranscriptional pre-rRNA processing and affects the global hierarchy of ribosome biogenesis. *RNA*, **22**, 852–866.

122. Gamalinda,M. and Woolford,J.L. Jr. (2014) Deletion of L4 domains reveals insights into the importance of ribosomal protein extensions in eukaryotic ribosome assembly. *RNA*, **20**, 1725–1731.

123. Pillet,B., García-Gómez,J.J., Pausch,P., Falquet,L., Bange,G., de la Cruz,J. and Kressler,D. (2015) The dedicated chaperone Acl4 escorts ribosomal protein Rpl4 to its nuclear pre-60S assembly site. *PLoS Genet.*, **11**, e1005565.

124. Talkish,J., Campbell,I.W., Sahasranaman,A., Jakovljevic,J. and Woolford,J.L. Jr. (2014) Ribosome assembly factors Pwp1 and Nop12 are important for folding of 5.8S rRNA during ribosome biogenesis in *Saccharomyces cerevisiae. Mol. Cell. Biol.*, **34**, 1863–1877.

125. Lebreton,A., Rousselle,J.C., Lenormand,P., Namane,A., Jacquier,A., Fromont-Racine,M. and Saveanu,C. (2008) 60S ribosomal subunit assembly dynamics defined by semi-quantitative mass spectrometry of purified complexes. *Nucleic Acids Res.*, **36**, 4988–4999.

126. Shimoji,K., Jakovljevic,J., Tsuchihashi,K., Umeki,Y., Wan,K., Kawasaki,S., Talkish,J., Woolford,J.L. Jr. and Mizuta,K. (2012) Ebp2 and Brx1 function cooperatively in 60S ribosomal subunit assembly in *Saccharomyces cerevisiae. Nucleic Acids Res.*, **40**, 4574–4588.

127. Granneman,S., Petfalski,E. and Tollervey,D. (2011) A cluster of ribosome synthesis factors regulate pre-rRNA folding and 5.8S rRNA maturation by the Rat1 exonuclease. *EMBO J.*, **30**, 4006–4019.

128. Konikkat,S., Biedka,S. and Woolford,J.L. Jr. (2017) The assembly factor Erb1 functions in multiple remodeling events during 60S ribosomal subunit assembly in *S. cerevisiae. Nucleic Acids Res.*, **45**, 4853–4865.

129. Pestov,D.G., Stockelman,M.G., Strezoska,Z. and Lau,L.F. (2001) *ERB1*, the yeast homolog of mammalian *Bop1*, is an essential gene required for maturation of the 25S and 5.8S ribosomal RNAs. *Nucleic Acids Res.*, **29**, 3621–3630.

130. Tang,L., Sahasranaman,A., Jakovljevic,J., Schleifman,E. and Woolford,J.L. Jr. (2008) Interactions among Ytm1, Erb1, and Nop7 required for assembly of the Nop7-subcomplex in yeast preribosomes. *Mol. Biol. Cell*, **19**, 2844–2856.

131. Oeffinger,M., Leung,A., Lamond,A., Tollervey,D. and Lueng,A. (2002) Yeast Pescadillo is required for multiple activities during 60S ribosomal subunit synthesis. *RNA*, **8**, 626–636.

132. Oeffinger,M. and Tollervey,D. (2003) Yeast Nop15p is an RNA-binding protein required for pre-rRNA processing and cytokinesis. *EMBO J.*, **22**, 6573–6583.

133. Fatica,A., Oeffinger,M., Tollervey,D. and Bozzoni,I. (2003) Cic1p/Nsa3p is required for synthesis and nuclear export of 60S ribosomal subunits. *RNA*, **9**, 1431–1436.

134. Dunbar,D.A., Dragon,F., Lee,S.J. and Baserga,S.J. (2000) A nucleolar protein related to ribosomal protein L7 is required for an early step in large ribosomal subunit biogenesis. *Proc. Natl. Acad. Sci. U.S.A.*, **97**, 13027–13032.

135. Gadal,O., Strauss,D., Petfalski,E., Gleizes,P.E., Gas,N., Tollervey,D. and Hurt,E. (2002) Rlp7p is associated with 60S preribosomes, restricted to the granular component of the nucleolus, and required for pre-rRNA processing. *J. Cell Biol.*, **157**, 941–951.

136. Adams,C.C., Jakovljevic,J., Roman,J., Harnpicharnchai,P. and Woolford,J.L. Jr. (2002) *Saccharomyces cerevisiae* nucleolar protein Nop7p is necessary for biogenesis of 60S ribosomal subunits. *RNA*, **8**, 150–165.

137. Lo,K.Y., Li,Z., Bussiere,C., Bresson,S., Marcotte,E.M. and Johnson,A.W. (2010) Defining the pathway of cytoplasmic maturation of the 60S ribosomal subunit. *Mol. Cell*, **39**, 196–208.

138. Fernández-Pevida,A., Kressler,D. and de la Cruz,J. (2015) Processing of preribosomal RNA in *Saccharomycescerevisiae. Wiley Interdiscip. Rev. RNA*, **6**, 191–209.

139. Esakova,O., Perederina,A., Quan,C., Berezin,I. and Krasilnikov,A.S. (2011) Substrate recognition by ribonucleoprotein ribonuclease MRP. *RNA*, **17**, 356–364.

140. Lygerou,Z., Allmang,C., Tollervey,D. and Séraphin,B. (1996) Accurate processing of a eukaryotic precursor ribosomal RNA by ribonuclease MRP in vitro. *Science*, **272**, 268–270.

141. Burlacu,E., Lackmann,F., Aguilar,L.C., Belikov,S., Nues,R.V., Trahan,C., Hector,R.D., Dominelli-Whiteley,N., Cockroft,S.L., Wieslander,L. *et al.* (2017) High-throughput RNA structure probing reveals critical folding events during early 60S ribosome assembly in yeast. *Nat. Commun.*, **8**, 714.

142. Peña,C., Schütz,S., Fischer,U., Chang,Y. and Panse,V.G. (2016) Prefabrication of a ribosomal protein subcomplex essential for eukaryotic ribosome formation. *eLife*, **5**, e21755.